Neuroscience Letters 717 (2020) 134673

Contents lists available at ScienceDirect

Neuroscience Letters

journal homepage: www.elsevier.com/locate/neulet

Review article

Mechanical regulation of oligodendrocyte biology

Ekta P. Makhija[a,b,1], Daniela Espinosa-Hoyos[a,c,1], Anna Jagielska[a,d,*,1], Krystyn J. Van Vliet[a,b,d,e,*]

[a] BioSystems & Micromechanics (BioSyM) Interdisciplinary Research Group, Singapore-MIT Alliance for Research & Technology (SMART) CREATE, Singapore 138602
[b] Critical Analytics for Manufacturing Personalized-Medicine (CAMP) Interdisciplinary Research Group, Singapore-MIT Alliance for Research & Technology (SMART) CREATE, 138602, Singapore
[c] Department of Chemical Engineering, Massachusetts Institute of Technology, Cambridge, MA 02139 USA
[d] Department of Materials Science & Engineering, Massachusetts Institute of Technology, Cambridge, MA 02139 USA
[e] Department of Biological Engineering, Massachusetts Institute of Technology, Cambridge, MA 02139 USA

ARTICLE INFO

Keywords:
Oligodendrocytes
Oligodendrocyte progenitor cells
Myelination
Mechanobiolgy
Mechanotransduction
Brain mechanics

ABSTRACT

Oligodendrocytes (OL) are a subset of glial cells in the central nervous system (CNS) comprising the brain and spinal cord. The CNS environment is defined by complex biochemical and biophysical cues during development and response to injury or disease. In the last decade, significant progress has been made in understanding some of the key biophysical factors in the CNS that modulate OL biology, including their key role in myelination of neurons. Taken together, those studies offer translational implications for remyelination therapies, pharmacological research, identification of novel drug targets, and improvements in methods to generate human oligodendrocyte progenitor cells (OPCs) and OLs from donor stem cells *in vitro*. This review summarizes current knowledge of how various physical and mechanical cues affect OL biology and its implications for disease, therapeutic approaches, and generation of human OPCs and OLs.

1. Introduction

Oligodendrocytes (OL) are a glial cell type that develops and functions in the complex microenvironment of the surrounding central nervous system (CNS) tissue comprising the brain and spinal cord. This environment provides multiple biochemical and physical cues that collectively regulate OL biology and function, including the complex OL function of neuron myelination. While the role of biomolecules including soluble factors, extracellular matrix (ECM) components, cell surface ligands and receptors has been studied extensively, the role of mechanical cues in OL biology is a much more recent field of active exploration. Growing experimental evidence shows that most stages of OL development, from neural stem cells to OL precursors to mature myelinating OLs, are responsive to external mechanical cues. Stimuli such as tissue or ECM stiffness, topography, mechanical strain, and macromolecular crowding affect OL lineage cells' migration, proliferation, differentiation and axon myelination [1–9]. Like the biochemical environment, this mechanical niche exhibits changes during organism development, aging, and disease. Consequently, mechanical cues within the normal physiological range can regulate OL differentiation and myelination, but these processes can also be disrupted when mechanical cues deviate beyond the normal range to define a pathological mechanical environment. The paucity of drug discovery for OL-related pathologies suggests incomplete understanding of OL and myelin biology.

By characterizing the mechanical niche in health and disease, and understanding its consequences for OL biology and function, we may identify new avenues to develop effective therapies for OL and myelin related diseases. Nevertheless, the mechanical niche in the nervous system remains largely unexplored, in part due to technical challenges in accurate measurement and recapitulation of CNS tissue and cell mechanical properties. Non-invasive methods that allow mechanical analysis of CNS tissue *in vivo*, such as magnetic resonance elastography (MRE), have spatial limitations and confer indirect estimates of mechanical properties; access to fresh CNS tissue from humans is limited; and animal models do not represent fully the mechanical properties of human healthy and diseased neuronal tissue. In addition, neural tissue is among the most compliant (*i.e.*, least stiff) tissues in the body, presenting challenges for accurate mechanical characterization of intact, hydrated tissues and cells in near-physiological conditions that

* Corresponding authors at: Singapore-MIT Alliance for Research & Technology (SMART) CREATE, Singapore 138602 and Massachusetts Institute of Technology, Cambridge, MA 02139 USA.
E-mail addresses: aj58@mit.edu (A. Jagielska), krystyn@mit.edu (K.J. Van Vliet).
[1] These authors contributed equally to this work.

https://doi.org/10.1016/j.neulet.2019.134673
Received 17 June 2019; Received in revised form 25 November 2019; Accepted 1 December 2019
Available online 12 December 2019
0304-3940/ Published by Elsevier B.V.

maintain structure that gives rise to those unique mechanical properties. Contact mechanics-based approaches including atomic force microscopy-enabled indentation, impact indentation, and pressure-induced cavitation have facilitated increasing access to elastic and viscoelastic properties of CNS tissue and cells, for both healthy and pathological state. However, those data reinforce the need for new models and tools to study the effects of mechanical and physical cues in nervous system cells such as OLs.

Here, we discuss current knowledge about the mechanical niche in the CNS in health and disease and the effects of mechanical cues on OL biology and axon myelination. We review the models and tools that have enabled mechanical studies of tissues and cells, the current understanding of mechanotransduction mechanisms in the OL lineage, and how these can be explored for the development of therapies for demyelinating diseases. Finally, we briefly discuss outstanding questions about the neuroglial mechanical niche and future directions in this field.

2. Mechanical cues in the CNS

The tools used to measure the mechanical properties of CNS tissue and cells depend on the specimen size (molecular, cellular, tissue level) and state (*in vitro, ex vivo, in vitro*). MRE [10] is a non-invasive macroscopic *in vivo* imaging technique that extracts mechanical properties of living tissue by applying shear waves and recording their propagation. Instrumented indentation [11], [12], impact indentation [11] [13], and macroscale rheometry [11], [14] [15], are *ex vivo* and *in vitro* techniques for characterization of cell and tissue stiffness. Depending on experimental design parameters including maximum applied strain and strain rate, these approaches can be used to quantify the elastic, viscoelastic, and poroelastic properties over length scales ranging from nanometers (subcellular) to centimeters (tissue or organ scale). The CNS contains some of the most mechanically compliant tissues and cells in the body, meaning that the mechanical stresses required to deform this tissue to a given strain (normalized displacement) are much lower than those required to deform mineralized bone tissue to the same strain magnitude. Colloquially, the term “soft” is often used to describe imprecisely the mechanical deformation and properties of brain tissue. In material mechanics, “soft” implies that the material undergoes plastic or *permanent* deformation at relatively low applied stresses; the opposite of soft materials are hard materials, in which permanent deformation requires relatively high applied stress. However, the term “compliant” describes elastic or *reversible* deformation at relatively low stresses; the opposite of compliant is stiff, and so this relative mechanical property can be described colloquially as stiffness. As the response of brain tissue under the small strains applied by common measurement techniques is reversible and recoverable, we refer to brain tissue as “compliant” as compared with mineralized bone tissue (whereas others may call the same relative comparison “soft”), because of the relatively lower stiffness of brain tissue. Others may also refer to stiffer materials as “rigid,” but in material mechanics this term implies infinite stiffness or resistance to deformation. Stiffness may be reported as a measured mechanical property such as a shear elastic modulus G or Young’s elastic modulus E, in units of N/m^2 or Pa.

Reported shear elastic and Young’s elastic moduli of healthy brain and spinal cord tissue span three orders of magnitude (10^{-1} – 10^{+1} kPa) [16–42]. Differences have been reported across brain matter regions, sex, species and modes of mechanical deformation [28], [41–43]. The wealth of deformation modes (tension, compression, shear), time scales and length scales (molecular, cellular, tissue level); specimen identity (species, donor, sex, and age), state (*in vivo, ex vivo, post mortem*), and biological tissue processing (fresh, frozen, chemically fixed); and environmental measuring conditions all affect the magnitudes, trends, and reproducibility of reported mechanical properties [9], [29], [43–48]. Overall, changes in brain tissue mechanical properties may be the correlate, cause, driving force, or accelerator of disease and developmental processes [26]; a consequence or adaptation mechanism to disease [49] and aging [50]; and may be used as a marker for disease detection or progression [51].

2.1. Mechanical cues: cellular interfaces, ECM and the vasculature

The mechanical landscape of the CNS has the potential to impact OL biology through physical interfaces at various length scales and indirect mechanisms. Neuronal axons are compliant and behave nearly elastically under strains and strain rates anticipated *in vivo* [52]. During development, axons provide a physical path of migration for OLs from the neural tube to the brain and spinal cord [53–60]. During myelination, physical forces drive the expansion and wrapping of the myelin membrane around the circumference of axons [61]. Mechanical displacements and forces at the axon membrane, generated by the firing of action potentials [62], can influence the activity of mechanosensitive axonal ion channels [63] and result in transient changes in axon diameter, pressure, optical properties and heat transfer [62]. These changes may affect OL lineage cells interacting directly with axons through adhesion complexes. Astrocytes, another glial cell type, express laminins that interact with OL mechanosensing integrins to mediate OL survival *in vitro* [64], and also express the cell surface ligands n-cadherins that slow OL migration rate in astrocyte-rich regions [65], [66]. Gap junctions coupling astrocytes, OLs, and neurons are rich in connexins [67–69], some of which are mechanoresponsive [70], [71], suggesting that astrocyte-OL gap junctions may be susceptible to mechanical forces. This hypothesis is supported by the observation that alterations in gap junctions are characteristic of multiple sclerosis (MS) brain tissue lesions and experimental autoimmune encephalomyelitis (EAE) models of demyelination [72], and correlated with genetic myelin disorders such as Pelizaeus-Merzbacher-like disease [73].

Beyond intracellular and cell-cell interactions that can serve as mechanical stimuli to OLs, mechanical changes of the extracellular matrix may also act indirectly on OL lineage cells. The extracellular matrix (ECM) comprises ~20 % of brain tissue volume [74], and cell surface receptor interactions with ECM proteins mediate cell responses that act directly through the cytoskeleton [75]. Prior studies have shown that mechanical transformations of neurons, astrocytes and microglia are modulated by extracellular mechanics [76–83]. OLs also associate with the vasculature and extracellular matrix (ECM). OL lineage cells migrate along and interact with multiple blood vessels [84]. Wnt signaling mediates OPC-endothelial interactions [84], and is mechanically activated or regulated at least in the lungs [85] and bones [85]. Co-culture experiments also suggest that endothelial cell sensitivity to shear flow [86] may bias adult neural progenitor cell lineage fate [87]. That observation prompts speculation that disruption of vascular flow in traumatic brain injury (TBI) [88] may compromise neurogenesis or oligodendrogenesis and impair regeneration. Finally, transport of inhibitory or supporting vesicles and neurotransmitters through the extracellular space is also strongly dependent upon the extracellular environment [86], [89–91].

2.2. Changes in the CNS mechanical landscape in development, aging, and disease

The brain reorganizes during development [23] [92], and aging [93], [94]. CNS tissues are subjected continuously to mechanical strain, which is distributed throughout its substructures (*e.g.*, up to 10 % strain in the spinal cord during flexion, or as a result of arterial pulsation [95–98]). The developing spinal cord elongates to accommodate skeletal growth, and cell proliferation facilitates brain volumetric expansion and folding. At the cellular level, axon growth is a source of strain on the surrounding developing microenvironment. There have been many attempts to quantify the magnitude and type of mechanical forces involved in axonal growth and guidance, which can increase to 10^2 nN [95]. The mechanical stiffness of brain tissue changes temporally

Table 1
Summary of mechanical properties of central nervous system tissue in various pathological states or induced-disease models, as compared with healthy control tissue.

Condition	Species	Tissue type	Tissue sub-type	Age	Sex	Tissue processing	Technique	Property measured	Values	Biochemical changes	Reference
AD	Human	Brain	HPC	67-80y	F/M	*In vivo*	MMRE	Phase angle Magnitude complex shear modulus	0.43 ± 0.06 0.87 ± 0.15 kPa	Positive correlation with mean diffusivity, and decreased hippocampal volume in patient group	[103]
	Human	Brain (HC)	HPC	66-79y	F/M	*In vivo*	MMRE	Phase angle Magnitude complex shear modulus	0.51 ± 0.07 1.08 ± 0.19 kPa		
AD	Human	Brain	Global	Adult	F/M	*In vivo*	MRE	Shear modulus	2.40 ± 0.09 kPa	Negative correlation with imaging measures of disease severity	[104]
	Human	Brain (CN)	Global	Adult	F/M	*In vivo*	MRE	Shear modulus	2.51 ± 0.09 kPa		
AD	Human	Brain	Global	76-94y	F/M	*In vivo*	MRE	Shear modulus	2.13 ± 0.17 kPa	–	[105]
	Human	Brain (CN-)	Global	75-89y	F/M	*In vivo*	MRE	Shear modulus	2.40 ± 0.23 kPa		
	Human	Brain (CN+)	Global	73-93y	F/M	*In vivo*	MRE	Shear modulus	2.43 ± 0.25 kPa		
AD model	Mouse	Brain	Cortex	6-8m	–	*Ex vivo*, fresh	AFM	Elastic modulus	0.41 ± 0.10 kPa	Decreased myelin	[106]
	Mouse	Brain (HC)	Cortex	6-8m	–	*Ex vivo*, fresh	AFM	Elastic modulus	0.65 ± 0.14 kPa		
Demyelination (Cuprizone model)	Mouse	Brain	CC	12-14w	M	*Ex vivo*, fresh	AFM	Apparent elastic modulus	0.14 ± 0.02 kPa	Decreased myelin and increased hyaluronan in demyelinated white matter	[35]
	Mouse	Brain (HC)	CC	12-14w	M	*Ex vivo*, fresh	AFM	Apparent elastic modulus	0.22 ± 0.02 kPa		
Demyelination (Cuprizone model) †	Mouse	Brain	CC	5-6w	F	*In vivo*	MRE	Magnitude complex shear modulus	20 % increase	Positive correlation demyelination and phase angle, and increased cell density, fibronectin	[107]
	Mouse	Brain (HC)	CC	5-6w	F	*In vivo*	MRE	Magnitude complex shear modulus	–		
Demyelination (EAE model)	Mouse	Brain	–	–	–	*In vivo*	MRE	Storage modulus Loss modulus	5.31 ± 0.16 kPa 1.42 ± 0.34 kPa	Negative correlation with inflammation (CD3 expression)	[108]
	Mouse	Brain (HC)	–	–	–	*In vivo*	MRE	Storage modulus Loss modulus	6.10 ± 0.17 kPa 1.89 ± 0.10 kPa		
Demyelination (Lysolecithin model, acute)	Mouse	Brain	CC	12w	–	*Ex vivo, frozen, fixed*	AFM	Elastic modulus	4.34 ± 2.55 kPa	Decreased myelin	[109]
	Mouse	Brain (HC)	CC	12w	–	*Ex vivo, frozen, fixed*	AFM	Elastic modulus	12.01 ± 6.16 kPa		
Demyelination (Cuprizone model, acute)	Mouse	Brain	CC	8w	M	*Ex vivo, frozen, fixed*	AFM	Elastic modulus	8.28 ± 3.49 kPa	Decreased myelin	
	Mouse	Brain (HC)	CC	8w	M	*Ex vivo, frozen, fixed*	AFM	Elastic modulus	12.07 ± 0.27 kPa		
Demyelination (Cuprizone model, chronic)	Mouse	Brain	CC	8w	M	*Ex vivo, frozen, fixed*	AFM	Elastic modulus	16.32 ± 9.46 kPa	Decreased myelin, and increased GFAP, vimentin, CSPG and fibronectin	
	Mouse	Brain (HC)	CC	8w	M	*Ex vivo, frozen, fixed*	AFM	Elastic modulus	12.07 ± 3.12 kPa		
MS (SP) *	Human	Brain	Acute WM lesion	62, 64y	F	*Ex vivo, frozen, fixed*	AFM	Elastic modulus, normalized to NAWM	1.43 ± 1.41, 1.07 ± 1.39, 0.93 ± 1.65	Increased GFAP, vimentin and fibronectin in stiff (chronic) *versus* compliant (acute) lesions	
	Human	Brain	Chronic WM lesion	62, 64y	F	*Ex vivo, frozen, fixed*	AFM	Elastic modulus, normalized to NAWM	2.97 ± 6.06, 4.44 ± 7.02, 4.03 ± 7.10		
	Human	Brain (HC)	NAWM	62, 64y	F	*Ex vivo, frozen, fixed*	AFM	Elastic modulus	–		
MS (SP/PP)	Human	Brain	Paren-chyma	Adult	F/M	*In vivo*	MRE	Viscoelastic constant, α Viscoelastic constant, μ	0.28 ± 0.01 2.61 ± 0.48 kPa	–	[110]
	Human	Brain (HC)	Paren-chyma	Adult	F/M	*In vivo*	MRE	Viscoelastic constant, α Viscoelastic constant, μ	0.29 ± 0.01 3.28 ± 0.32 kPa		
MS (RR)	Human	Brain	Paren-chyma	Adult	F/M	*In vivo*	MRE	Viscoelastic constant, μ	3.03 ± 0.46 kPa	–	
	Human	Brain (HC)	Paren-chyma	Adult	F/M	*In vivo*	MRE	Viscoelastic constant, μ	3.55 ± 0.56 kPa		

(*continued on next page*)

Table 1 (*continued*)

Condition	Species	Tissue type	Tissue sub-type	Age	Sex	Tissue processing	Technique	Property measured	Values	Biochemical changes	Reference
MS (RR)	Human	Brain	Paren-chyma	22-50y	F	*In vivo*	MRE	Viscoelastic constant, μ	1.88 ± 0.26 kPa	–	[111]
				21-51y	M	*In vivo*	MRE	Viscoelastic constant, μ	1.86 ± 0.26 kPa		
	Human	Brain (HC)	Paren-chyma	18-55y	F	*In vivo*	MRE	Viscoelastic constant, μ	2.27 ± 0.31 kPa		
				21-59y	M	*In vivo*	MRE	Viscoelastic constant, μ	2.01 ± 0.27 kPa		
Parkinson's (dopamine depletion model) **	Mouse	Brain	HPC	8-10wk	F	*In vivo*	MRE	Storage modulus	4.61 ± 60.72 kPa	Positive correlation with neuronal density	[112]
	Mouse	Brain (dpi 6)	HPC	8-10wk	F	*In vivo*	MRE	Storage modulus	6.98 ± 1.02 kPa		
Parkinson's	Human	Brain	LN	52-74y	F/M	*In vivo*	MRE	Magnitude complex shear modulus	1.96 ± 0.22 kPa	Negative correlation with age and disease severity	[113]
	Human	Brain (HC)	LN	53-75y	F/M	*In vivo*	MRE	Magnitude complex shear modulus	2.10 ± 0.2 kPa		
Supra-nuclear palsy	Human	Brain	Global	64-76y	F/M	*In vivo*	MRE	Phase angle	0.17 ± 0.07		
								Magnitude complex shear modulus	1.68 ± 0.17 kPa		
	Human	Brain (HC)	Global	53-75y	F/M	*In vivo*	MRE	Phase angle	0.26 ± 0.04		
								Magnitude complex shear modulus	1.97 ± 0.18 kPa		
Stab injury (glial scar) †	Rat	Brain	Cortex	90d	–	*Ex vivo, fresh*	AFM	Elastic modulus	12-77 % decrease	Positive correlation with GFAP, collagen IV, vimentin, laminin	[31]
	Rat	Brain (HC)	Cortex	90d	–	*Ex vivo, fresh*	AFM	Elastic modulus	0.28 ± 0.23 kPa		
Tumor model	Mouse	Brain	Glio-blastoma	6w	F	*In vivo*	MRE	Storage modulus	4.80 ± 0.21 kPa	Positive correlation with tumor cell density and microvessel density	[114]
								Loss modulus	2.94 ± 0.19 kPa		
	Mouse	Brain	Glioma	6w	F	*In vivo*	MRE	Storage modulus	4.22 ± 0.14 kPa		
								Loss modulus	2.41 ± 0.14 kPa		
	Mouse	Brain (HC)	Paren-chyma	6w	F	*In vivo*	MRE	Storage modulus	5.89 ± 0.17 kPa		
								Loss modulus	4.36 ± 0.17 kPa		
Glioma	Human	Brain	Glioma	25.68y	F/M	*In vivo*	MRE	Magnitude complex shear modulus	2.27 ± 0.70 kPa	Negative correlation with tumor grade	[115]
	Human	Brain (HC)	NAWM	25-68y	F/M	*In vivo*	MRE	Magnitude complex shear modulus	3.3 ± 0.70 kPa		
	Human	Brain	Glioma, IDH1 mutation	25.68y	F/M	*In vivo*	MRE	Magnitude complex shear modulus	2.50 ± 0.60 kPa	–	
	Human	Brain (HC)	Glioma, WT	25-68y	F/M	*In vivo*	MRE	Magnitude complex shear modulus	1.6 ± 0.30 kPa		
Meningioma	Human	Brain	Tumor	–	–	*Ex vivo,* fresh	Indentation	Steady-state modulus	3.97 ± 3.66 kPa	–	[116]
	Mouse	Brain	Tumor	–	–	*Ex vivo,* fresh	Indentation	Steady-state modulus	7.64 ± 4.73 kPa		
	Mouse	Brain (HC)	–	–	–	*Ex vivo,* fresh	Indentation	Steady-state modulus	1.56 ± 0.75 kPa		
Ischemic stroke model	Mouse	Brain	IH	Adult	M	*Ex vivo, fixed*	UE	Shear modulus	3.85 ± 0.96 kPa	–	[117]
	Mouse	Brain	CH	Adult	M	*Ex vivo, fixed*	UE	Shear modulus	4.86 ± 1.79 kPa		
	Mouse	Brain (HC)	IC	Adult	M	*Ex vivo, fixed*	UE	Shear modulus	4.32 ± 1.44 kPa		
	Mouse	Brain (HC)	CH	Adult	M	*Ex vivo, fixed*	UE	Shear modulus	4.49 ± 1.32 kPa		
Normal pressure hydrocephalus	Human	Brain	Cerebrum	67-79y	F/M	*In vivo*	MRE	Shear modulus	2.64 ± 0.10 kPa	–	[24]
	Human	Brain (HC)	Cerebrum	67-80y	F/M	*In vivo*	MRE	Shear modulus	2.55 ± 0.10 kPa		

The studies summarized herein report differences in stiffness and viscoelasticity of central nervous system tissue in disease and disease models compared to healthy controls or adjacent tissue. The designation "HC" in this table refers to healthy control tissue. Values reported as mean ± standard deviation. All abbreviations in this extensive table are defined in Table 2. Only statistically significant differences ($p < 0.05$) are reported unless otherwise indicated (* no statistical analysis of comparison of healthy *versus* disease tissue.). † Exact values of mechanical properties not reported. ** Transient changes, compared to baseline values.

Table 2
Abbreviations of terms used to summarize an extensive range of studies of healthy *vs*. diseased brain tissue mechanics in Table 1.

Abbreviations	
HC	Healthy control
MRE	Magnetic resonance elastography
MMRE	Multifrequency-MRE
HPC	Hippocampus
F	Female
M	Male
d/w/y	Day/week/year
dpi	Days post injection
CN-	Amyloid-negative cognitively normal
CN +	Amyloid-positive cognitively normal
CN	Cognitively normal
AD	Alzheimer's
MS	Multiple Sclerosis
RR	Relapse Remitting
SP	Secondary Progressive
PP	Primary Progressive
WM	White matter
NAWM	Normal appearing white matter
CC	Corpus callosum
LN	Lentiform nucleus
UE	Ultrasound elastography
GFAP	Glial fibrillary acidic protein
CSPG	Chondroitin sulfate proteoglycans
IH	Ipsilateral hemisphere
CH	Contralateral hemisphere
WT	Wild type
AFM	Atomic force microscopy

* No statistical analysis of comparison of healthy *versus* disease tissue.
† Exact values of mechanical properties not reported.
** Transient changes, compared to baseline values.
Results from healthy controls (HC).

throughout development [99], and generally decreases with adult age [100], [101]. However, stiffening of aging rat brains has also recently been reported [102].

In pathological conditions that include Alzheimer's, Parkinson's, Multiple Sclerosis, cancer and injury, the viscoelastic properties of CNS tissue are altered, and stiffness changes by up to two orders of magnitude (Table 1, where HC indicates reported properties of healthy control tissue. All abbreviations in this extensive table are defined in Table 2). For example, the glial scar formed post-injury in the rat brain neocortex is more compliant (12–77% lower elastic modulus) than the uninjured tissue (0.28 kPa) [31]. In the murine model of demyelination, acute demyelinating lesions in the corpus callosum can be as much as two times more compliant (0.12 kPa) than the healthy tissue (0.24 kPa) [35], while chronic demyelinated lesions in the corpus callosum can be stiffer (*i.e.*, higher elastic modulus; 16.32 kPa) than the surrounding normal appearing tissue (12.07 kPa) [109]. Fig. 1 illustrates this relative comparison of healthy CNS tissue, glial scars, and chronic lesions. However, the above three examples also illustrate that the magnitude of stiffness reported in multiple studies may not agree well even among healthy control samples; this is attributable to variation in testing conditions as well as tissue sample preparation and preservation, even if the species and anatomical region of the tissue are conserved.

These pathological mechanical changes are often accompanied by biochemical changes that include myelin loss, accumulation of ECM components, and gliosis (Table 1). In CNS tissues that appear otherwise healthy, elastic and viscoelastic properties are also correlated with cell density and axon orientation [22], [112], [120], [121], acidosis [46], and myelin content [122]. After traumatic brain injury, axons bulge under compression and the myelin sheath surrounding the axons shrinks and swells [123]. In models of severe TBI, mechanical strain is associated with a cascade of damage to the mitochondria of cortical neurons, activation of reactive oxygen species, release of pro-apoptosis factors, and neuronal cell death [124]. The number of axons with functional deficit and damage to the surrounding OL also increase with the magnitude of macroscopic mechanical stretch [125], [126]. This is consistent with patterns of OL and axonal damage with severity of white matter injury. The microstructural deformations of axons of the adult guinea pig optic nerve and the developing chick embryo spinal cord subjected to macroscopic strain fields are consistent with a model in which axons and glia are uncoupled at low strain, and become gradually more coupled as the magnitude of stretch increases [127], [128]. The coupling becomes more pronounced with each developmental stage, plausibly reflecting developmental structural changes such as myelination [127], [129], or the evolving glia-neuron ratio with increasing brain mass. These studies also contribute to the evidence that axons throughout the CNS are tortuous [130]. Temporal increases in axonal tortuosity in response to dynamic strain have also been attributed to microtubule damage and reorganization [131], which has also been associated with axon stiffening [99].

3. Engineering tools to study mechanical cues *in vitro*

To understand the impact of the physical cues on the nervous system, it is instructive to control and mimic these cues in a laboratory setting. Diversity in the type and magnitude of mechanical cues across different parts of the CNS and across species poses a technological challenge for emulating those varying conditions *in vitro*. For such studies, it is not sufficient to span a range for a given cue (*e.g.*, span a threefold range of ECM shear elastic modulus G), but also to approximate the magnitude of those cues under study (*i.e.*, the specific values of G) with the corresponding magnitudes *in vivo*. This is because cell responses can vary nonmonotonically as a function of magnitude of a given cue (*e.g.*, biphasic response of cell migration velocity with ECM stiffness [278], [279]). Below, we summarize approaches to engineer mechanical cues *in vitro*.

3.1. Engineering stiffness

Nervous system tissue is among the most compliant tissues in the body, and its stiffness varies among species [280]. This low resistance to reversible deformation can be summarized most simply by comparison of elastic moduli measured under shear (shear elastic modulus, G) or uniaxial deformation (Young's elastic modulus, E). Murine tissue stiffness ranges from E of a few Pascals to ~1 kPa. Traditionally, *in vitro* neuronal cell culture has been conducted with CNS cells adhered to dishes comprised of polystyrene (*i.e.*, tissue culture plastic), an engineered polymer that is six orders of magnitude stiffer than neural tissue and therefore does not provide neural cells a mechanical cue *in vitro* that is similar to the *in vivo* environment. To match the very low stiffness of neural tissue, biocompatible substrata based on hydrogels of synthetic and/or natural polymers have been adopted or developed. These include polyacrylamide hydrogels (PAAm), polyethylene glycol (PEG), hexanediol diacrylate-PEG or HDDA-PEG, alginate, collagen, hyaluronic acid (HA), and gelatin based gels. CNS tissue stiffness shows also natural spatial variation [14] [35], among different parts of the CNS, and variation resulting from disease and aging.

However, in engineering such gels as mimics of tissue mechanical properties, it is important to be precise in stating the property that is varied, and to also match the magnitude of that property (or note that one is operating in a super- or sub physiological stiffness regime). Some of these polymers can be varied in stiffness by controlling the degree of polymer crosslinking, so that the dominant difference or cue among a set of polymer substrata is the elastic modulus. Jagielska et al. [5] adopted this approach for widely utilized PAAm gels to cover the range of physiological and pathological CNS stiffness values from $E \sim$ 0.1–70 kPa, demonstrating that OL biology including differentiation potential was modulated by substratum stiffness over this range. Specifically, that study covered the range of reported brain tissue E (0.1–1.0 kPa) and also exceeded it at the upper limit of 70 kPa. Urbanski et al. [9]

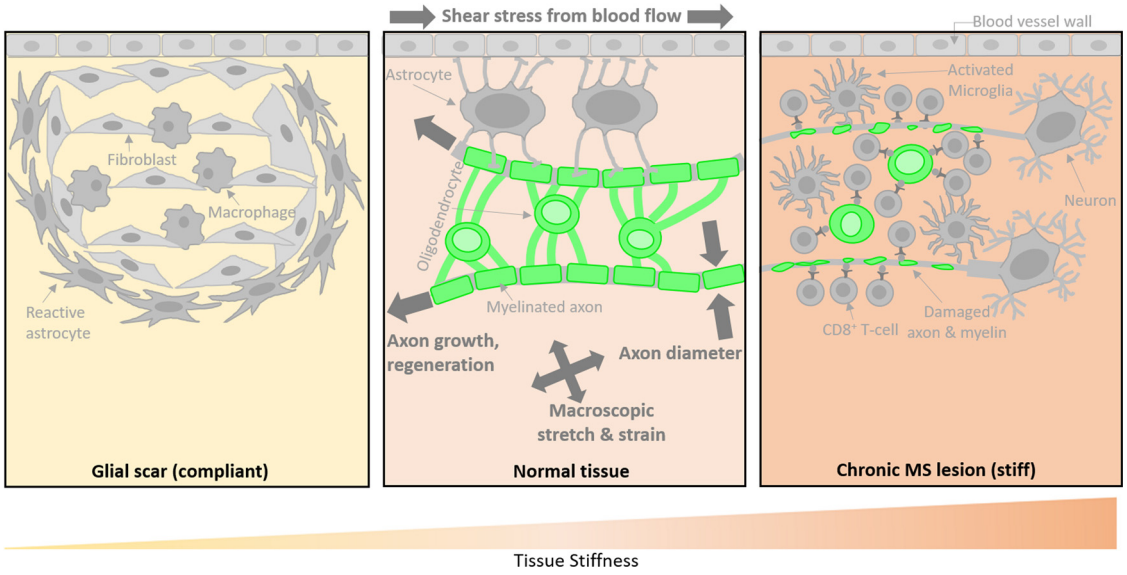

Fig. 1. CNS mechanical microenvironment in health and disease.
The mechanical properties of the CNS change with development, disease, and aging. Three different CNS tissue scenarios are depicted: a glial scar, a normal tissue, and a chronic MS lesion. Tissue stiffness is shown using the yellow-orange color map. Oligodendrocytes and myelin are shown in green. Normal CNS tissue includes dynamic mechanical cues arising from axon length and diameter changes, macroscopic strains, and shear force from blood flow. Glial scars formed after a CNS injury are more compliant than normal CNS tissue, lack axons, neurons, and oligodendrocytes, and include fibroblasts, macrophages, and reactive astrocytes [118]. Chronic MS lesions exhibit damaged myelin, axons, and oligodendrocytes, and include $CD8^+$ T-cells and activated microglia [119].

used similar PAAm gels to investigate OL biology on stiffness ranging 2–30 kPa, and in that sense the full range of stiffness exceeded that expected of at least healthy brain tissue. Recently, Segel et al. [102] used a pair of modified PAAm hydrogels as an attempt to mimic the mechanical changes that varied with animal age, in order to explain changes in OPC biology as a function of CNS aging. The stiffness of those two hydrogels differed approximately threefold to assess OPC response *in vitro*, and the stiffness of the brain tissue that the authors characterized in the same study differed approximately twofold. While that is a similar range of variation, it is not clear from the data presented whether the magnitudes of that *in vitro* stiffness cue actually matched or were even within an order of magnitude of the brain tissue stiffness reported in that same study. (Gel stiffness was reported as G of 0.4 or 1.3 kPa, which we convert to E of 1.2 or 3.9 kPa with an assumption of gel Poisson's ratio of 0.5 to provide context with above reports. However, the brain tissue stiffness was reported simply as "average stiffness" of 0.24 or 0.48 kPa, which may have been G or apparent bulk elastic modulus K. If the former, then E of brain tissue at those two animal ages would be 0.72 or 1.44 kPa, so the upper range of brain tissue stiffness was the lower range of gel stiffness; if the latter, then E at those brain tissue ages would be 0.18 or 0.36 kPa and would differ by an order of magnitude from the gel stiffness range.) Thus, the reported *in vitro* trends should not be conflated or assumed *a priori* to be predictions of *in vivo* response of OPC if the magnitudes of the engineered and *in vivo* environments differ substantially. Li et al. [132] developed injectable hydrogels containing gelatin and hyaluronic acid crosslinked with PEG diacrylate (PEGDA), which covered a range of elastic modulus from 0.0048 to 1.60 kPa. These hydrogels were studied as potential medium to increase remyelination by OPCs transplanted into a demyelinating lesion environment.

Contact mechanics-based studies of neural tissue revealed that spatial variation of stiffness occurs also at smaller length scales of ~50 – 100 μm [9], [11], [35], [40], and approaching that of cell length scales. Achieving this high resolution of stiffness variation in the substratum material is challenging, but could be enabled by additive techniques such as 3D printing materials of varying stiffness [2] or by stereolithography-based curing of polymers to various degrees through masks of varying grayscale values [133]. Indeed, Espinosa-Hoyos et al. [2] developed novel HDDA-PEG hydrogels, for which stiffness could be tuned from 0.1–150 kPa through polymer composition and stereolithography-based polymer curing. This material was used to develop artificial axons – 3D printed free-spanning structures designed to mimic the cylindrical geometry and mechanical stiffness of biological axons. By tuning artificial axon stiffness between healthy (0.4 kPa) and pathological values (140 kPa), Espinosa-Hoyos et al. [2] demonstrated that artificial axon stiffness can affect the extent of myelination by OLs that can bind to and wrap the 3D-printed, engineered polymer.

3.2. Engineering strain

Neural cells are subjected to various mechanical strains, including tension, compression, and shear, both in healthy development as well as a result of external mechanical trauma such as traumatic brain or spinal cord injuries. These strains are estimated to vary from few percent [134] to over 100 % (for example, in the case of tissue swelling [135]). Devices available commercially (*e.g.*, Flexcell devices, Flexcell Int. Corp.) or custom-designed by academic researchers allow for application of strain schedules of varying magnitudes, modes, and duration. Strain is typically applied to adherent cells such as OLs and their progenitor cells (OPCs) indirectly by straining the substratum to which those cells are adhered. Jagielska et al. [4] and Makhija et al. [7] applied static, uniaxial tensile strain of 10 % of various durations to OPCs, to study strain effect on their proliferation and differentiation. Strain was applied by stretching custom-made silicone elastomer (polydimethylsiloxane, PDMS) culture plates on which cells were grown, adapting a custom device developed initially for study of vascular endothelial cells [136]. The design of the plates and the stretcher ensured uniform strain in all parts of the plate, with minimal border effects, and full transfer of strain to the cells. Shimizu et al. [137] applied 15 % uniaxial tensile strain to OPCs by stretching (8 min duration) silicone sheets on which cells were grown, to investigate the role of YAP in transduction of strain. In the same work, effect of shear strain on YAP-mediated mechanotransduction was studied, where shear stress was applied by overnight rotation of flasks with media. Hernandez et al. [3] applied acute contraction to OPCs (*i.e.*, rapid removal of strain applied prior to cell seeding and adhesion), to study effects on OPC

differentiation and mechanotransduction mechanisms. Although studies of OPCs and OLs reported to date have been carried out in two-dimensional (2D) cell culture, extension to three-dimensional strain states or culture settings is feasible in artificial axon settings, within gels, or other constructs.

3.3. Engineering topography and spatial constraints

Neural tissue exhibits complex three-dimensional topography defined by neural cells and ECM. Despite this fact, majority of *in vitro* studies of neurons and neuroglia are carried out in 2D culture for its simplicity of handling and imaging, as well as relatively easier image analysis. On the other end of the complexity spectrum for *in vitro* studies are co-cultures (*e.g.*, OPCs co-cultured with neurons) or organotypic tissue slice cultures [138]. Such biological constructs provide greater biofidelity, but with the tradeoff of high spatial complexity and intrinsically diverse variation among samples, batches, and donors; these features make data analysis and interpretation, as well as experimental design, difficult. Therefore, reproducible and reductionist engineered systems that can mimic geometric features of the CNS, together with mechanical properties of CNS features that modulate neuroglia cell response, are of great interest. Influence of geometric features such as cell density was demonstrated by Rosenberg at al. [8]. In that work, neighboring neural cells in the OPC environment were mimicked with 20 μm polystyrene spheres, to demonstrate that critical spatial constraints were necessary to induce OPC differentiation grown in co-culture with axons. That experiment was repeated later in work of Hernandez at al [3], to show that the OPC differentiation enhanced by high microsphere density corresponded with increased number of chromocenters in cell nuclei, indicating mechanotransduction of spatial density-induced cues to the nucleus with resulting chromatin changes.

One critical topographical feature in the OPC environment are neuronal axons, with which OPCs closely interact to wrap and maintain myelin sheaths around the axon circumference. Detailed study of myelination is not possible without this 3D feature of the culture environment, as axon myelination by OLs is an inherently three-dimensional phenomenon. Some topographies can be designed for purposes other than mimicking physiological conditions. Mei at al. [139] developed arrays of glass cones as an assay for high throughout myelination assessment. Although those cones did not resemble axon geometry and did not provide physiological stiffness, they provided a shape to which OL processes could adhere and begin to encircle with MBP, and thus enabled fast relative quantification of myelin production that was suggestive of myelination ensheathment.

Rosenberg et al. [8] demonstrated that even without dynamic axon signaling, OPCs can myelinate cylindrical axons, suggesting that the geometrical cues are sufficient to support if not induce myelination. They demonstrated this potential in the absence of neuron firing by chemically fixing DRG neurons with paraformaldehyde and plating OPCs on top of these biochemically inactive axons. Subsequent studies demonstrated that replacing axons with synthetic cones or cylindrical fibers of microscale diameter also resulted in myelin basic protein (MBP)-production by murine cells [1], [2], [6], [134], [140]. The potential for OLs to produce this key myelin sheath component and deposit it at the surface of the synthetic fiber – and at least in some cases exhibit a morphology that appeared like wrapping of the MBP positive membrane around the curved features as would be expected in biological myelination – has been reported for various materials including glass, polystyrene, carbon nanotubes, PLLA (poly-L-lactic acid), PCL (polycaprolactone), and HDDA-star-PEG. Those observations indicate that myelin formation and deposition to at least start to ensheath axon-like structures is an intrinsic feature of OL, and does not require dynamic biological or electrochemical signals from axon. However, axons regulate fine features of myelin, such as myelinated segment length and thickness of compacted (multilayered) myelin sheaths, *via* physical and chemical signals to degrees that have not yet been understood fully or recapitulated *in vitro*. To date, the research community has developed basic tools and observations. Lee at al. [6] used electrospun polystyrene fibers with diameter range of 0.2–4 μm to demonstrate that OLs preferentially myelinate fibers of larger diameter, indicating that mechanical cues can govern the diameter-dependence of myelination. Bechler et al. [1] used PLLA fibers with diameters 2–4 μm to show that length of myelin internodes is regulated by fiber diameter, and that OPCs possess intrinsic propensity to generate different myelin sheet length spans depending on the cells' *in vivo* origin. Espinosa-Hoyos et al. [2] generated the first axon-like fibers that combined axon geometric features (diameter and unsupported length span) with low mechanical stiffness matching that of biological axons ($E \sim 0.4$ kPa). In contrast to PLLA or PCL fibers exhibiting MPa-scale elastic moduli or polystyrene or glass features exhibiting at least GPa-scale elastic moduli, those 3D-printed fibers comprised HDDA-starPEG affording E ranging ~ 0.4 – –140 kPa. Those artificial axons were used to demonstrate the influence of axon mechanical stiffness on OL myelination.

4. Implications for OL biology

4.1. Mechanical cues affect OL differentiation and myelination

Several studies in the last decade have measured OL differentiation and myelination as a function of mechanical cues. However, even when identification of trends appear reproducible within a given study, comparison of the conclusions among multiple studies illustrates apparent conflict (Fig. 2). For example, within a given study or others' summaries of a study, it may be claimed that a cell response is elicited by "stiffer" or "more compliant" substrata, and on "smaller" or "larger"

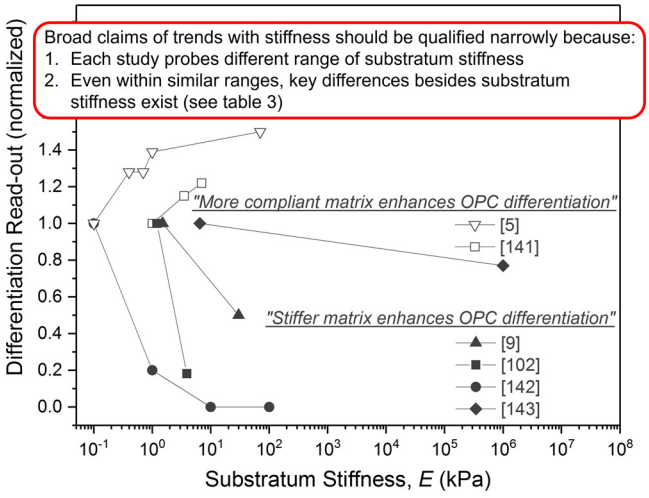

Fig. 2. Generalized statements, such as either the stiffer or the more compliant matrix enhances OL differentiation, are misleading.
Comparison of six studies that measured effect of substratum stiffness on OL differentiation. The horizontal axis represents the range of substratum stiffness (in logarithmic scale so as to fit all studies on the same graph). The vertical axis represents the read-out of OL differentiation used in that particular study, *i.e.*, either percentage of MBP + cells, percentage of RIP + cells, or MBP fluorescence intensity per cell. The read-out from each study has been normalized with its read-out at lowest substratum stiffness in that study. Note two features that make broad generalizations misleading. First, studies conducted within the same range of substratum stiffness can identify opposite trends in OL differentiation enhancement (*e.g.*, [5] and [142]). Second, studies that operate over a partially overlapping range of stiffness (*e.g.* [141], and [143]) conflict in trend, and this may be because the cell response over that entire range is non-monotonic or biphasic. Of course, overinterpretation of these data comparisons is not warranted because all of these studies varied in at least one important condition (*e.g.*, they used different substratum material, ECM ligand coating, starting cell type (NSC or OPC), or read-out of differentiation. See Table 3 for more details).

diameter fibers. However, this use of relative terms can be misleading when overly generalized, or when the range of mechanical stiffness studied, or when the magnitude of that cue or of other potential cues such as soluble factors or tethered ligand density, is not also considered explicitly. Fig. 2 compares six studies, and illustrates two features that make broad generalizations of mechanically modulated OPC differentiation misleading. First, studies conducted within the same range of substratum stiffness can identify opposite trends in OL differentiation enhancement (*e.g.*, comparison of data reported in Refs. [5] and [142]). Second, studies that operate over a partially overlapping range of stiffness (*e.g.*, comparison of data reported in Refs. [141] showing increasing differentiation with increasing substratum stiffness and [143] showing decreasing differentiation with further increase in substratum stiffness) conflict in trend. Again, this caution is in part because many cell responses including cell-matrix interactions are known to change non-monotonically with the magnitude of a cue, and so signaling effects and cell response trends cannot be considered *a priori* to trend monotonically.

Of course, overinterpretation of these studies compared in Fig. 2 is not warranted because all of these studies varied in at least one important condition (*e.g.*, they used different substratum material, ECM ligand coating, starting cell type (NSC or OPC), or read-out of differentiation. See Table 3 for more details). The effects of various mechanical cues on OPC differentiation and myelination are summarized in Table 3. Below, we summarize our key findings from comparing the collection of a broader range of studies summarized in Table 3.

4.1.1. Effects of mechanical cues depend on the cell stage in lineage progression

For example, adult rat neural stem cells (NSC) yielded a larger percentage of MBP + cells on more compliant 0.1 kPa substrata in one study [142], while neonatal rat OPCs yielded a larger percentage of MBP + cells on stiffer 1−70 kPa substrata compared to 0.1 kPa in another study [5]. Although in both studies the same substratum materials (polyacrylamide) and stiffness range were used, an opposite trend of differentiation response to stiffness was observed. While this contrast may be attributable to the difference in developmental age of the cell sources in these studies, though this cannot be inferred without first considering other potential differences in cell preparation, material substrata preparation and properties, or other protocol differences that may affect OPC differentiation to the stage of detectable MBP production.

4.1.2. Cell response to mechanical cues may vary with cue magnitude range

Two studies examined differentiation of rat OPCs into MBP + cells on polyacrylamide substrata of varying stiffness. In the first study [5], substrata with *E* of 0.1, 0.4, 0.7, 1 and 70 kPa stiffness and PDL functionalization were used. OPC differentiation was enhanced on stiffer substrata (18 %, 23 %, 23 %, 25 %, and 27 % MBP + cells, respectively). In the second study [9], substrata with *E* of 1.5 and 30 kPa were used with Matrigel™ coating; those authors reported that OPC differentiation was inhibited on the stiffer substratum (8 %, and 4 % MBP + cells, respectively). The different conclusions of the above studies could

Table 3
Summary of various studies using mechanical cues for OL differentiation and myelination. [144–150,141,142,151,152,9,5,143,102,4,8,153,6,154].

Starting cell stage	End cell stage / Read-out		Mechanical cue parameters		Chemical cue parameters		Reference
			Duration	Type & Magnitude	Substratum / Scaffold Material	ECM protein / Signalling Molecule	
Pre-NSC							
mouse ESC	4	15% MBP+ cells	14 days	3D gel scaffold	Hyaluronic Acid	- / Retinoic Acid	[144]
human ESC	1	69% NKX2.2+ cells	18 days	3D gel scaffold	PNIPAAm-PEG	- / Retinoic Acid + Smoothened Agonist	[145]
human ESC	2	Olig-1 mRNA (gel-based)	7 days	Micropatterns (wells: 2 μm, pillars: 1 μm)	PDMS	Poly-L-Ornithine followed by laminin / -	[146]
human USC	4	15% MBP+ cells	30 days	between 2 coverslips	DETA-coated glass	- / Neropinephrine	[147]
NSC							
mouse embryo NSC	2	3.9, 3.3 fold NG2+ cells compared to glass	4 days	Electrospun fibers (random and aligned: 550 nm)	Polycaprolactone (PCL)	Brain derived neutrophic factor / -	[148]
adult rat NSC	3	56%, 21% RIP+ cells	5 days	Electrospun fibers (random: 283, 749 nm)	Polyethersulfone	- / Retinoic Acid	[149]
mouse embryo NSC	3	1.5%, 0.6%, 2.6% O4+ cells	5 days	Mechanical strain (0%, 10%, 10%-prestrain)	Silicone elastomer	Laminin / -	[150]
adult rat NSC	3	59%, 68%, 72% RIP+ cells	8 days	Substratum Stiffness (E < 1, 3.5, 7 kPa)	Methylacrylamide Chitosan	Laminin / -	[141]
adult rat NSC	4	10%, 2%, 0%, 0% MBP+ cells	6 days	Substratum Stiffness (E = 10^{-1}, 10^{0}, 10^{1}, 10^{2} kPa)	Polyacrylamide	Laminin / -	[142]
adult rat NSC	4	25% MBP+ cells 32% Olig2+ cells	6 days	Electrospun fibers (random: 200-300 nm)	PCL fibers coated with Graphene Oxide	Laminin / -	[151]
human NSC	2	4 fold Olig2 mRNA compared to flat substrate	5 days	Micropatterns (grooves: 1.5 μm, pores: 10 nm)	Poly(styrene-b-methyl methacrylate)	Fibronectin / -	[152]
OPC							
neonatal rat OPC	4	8%, 4% MBP+ cells	2 days	Substratum Stiffness (E = 1.5, 30 kPa)	Polyacrylamide	Matrigel / -	[9]
neonatal rat OPC	4	18%, 23%, 23%, 25%, 27% MBP+ cells	3 days	Substratum Stiffness (E = 0.1, 0.4, 0.7, 1, 70 kPa)	Polyacrylamide	Poly-D-Lysine / -	[5]
neonatal rat OPC	4	1.3 fold MBP fluorescence intensity per cell compared to plastic	5 days	Substratum Stiffness (E = 6.5 kPa)	Polyacrylamide	Poly-D-Lysine & Merosin / -	[143]
adult rat OPC	4	55%, 10% MBP+/SOX10+ cells	5 days	Substratum Stiffness (E = 1.2, 3.9 kPa)	Polyacrylamide	Laminin / -	[102]
neonatal rat OPC	4	10%, 30% MBP+ cells	5 days	Mechanical strain (0%, 10%)	Polydimethylsiloxane	Fibronectin / -	[4]
neonatal rat OPC	4	2, 20, 65, 75 MBP+ cells / mm^2	5 days	Cell plating density (1, 2, 4, 8 million per coverslip)	DRG neurons on glass coverslips	- / -	[8]
neonatal rat OPC	4	11%, 10%, 17% MBP+ cells among Olig2+ cells	7 days	Electrospun fibers (aligned: 300, 700, 2000 nm)	PCL fibers coated with 3,4-dihydroxy-L-phenylalanin	Laminin / microRNA-219/338	[153]
neonatal rat OPC	5	5%, 60% cells wrapped around fibers	15 days	Electrospun fibers (aligned: 400, 4000 nm)	Poly L-lactic acid	Poly-L-lysine / -	[6]
human OPCs	2	A2B5+ and Olig2+ cells (image-based)	8 days	3D nanofibrous scaffold	Fibrinogen and thrombin	- / -	[154]

Color-Code:	Cell end stage numbering	
murine	1	Pre-OPC: NKX2.2
human	2	OPC: NG2, A2B5, Olig1, Olig2
	3	Immature OL: O4, RIP
	4	Mature OL: MBP
	5	Myelinating OL: Wrapping

Color-Code:
Substratum Stiffness
Electrospun fibers
Mechanical strain (0%, 10%)
3D scaffold
Micropatterns
Others

These studies are classified into three groups (pre-NSC, NSC, OPC), based on the differentiation stage of the starting cell type. Within each of the three groups, studies are further delineated based on the author-reported quantified metric (read-out) for differentiation outcome. Most studies used one of the five common types of mechanical or physical cues (substratum stiffness, mechanical strain, 3D scaffold material selection, electrospun fiber material/diameter, and micropatterns).

be rationalized by at least three factors. First, the differentiation efficiency could depend on substratum stiffness in a non-monotonic way, *i.e.*, it may increase or decrease for different range of stiffness, such as a biphasic response (Fig. 2). Second, the differentiation efficiency could also vary with adhesive ligand type. Third, it is possible that the Matrigel coating was sufficiently thick to moderate or obscure the mechanical cue of the underlying polyacrylamide [155].

4.1.3. Chemical cues modulate cell responses to mechanical cues

The chemical cues provided by the ECM proteins and the culture medium (signaling molecules such as growth factors, differentiation inducers, and transcription factors) are known regulators of OL differentiation and myelination [156–158]. For example, when functionalized on tissue-culture polystyrene substrata, the ECM ligands fibronectin, laminin, or PDL all showed approximately three-fold higher differentiation of embryonic stem cells to OL-lineage cells compared to uncoated plastic substrata [144]. However, when applied together with mechanical cues, the chemical cues may elicit differential cell responses. For example, in the presence of 10 % mechanical strain, only fibronectin- or laminin- but not PDL-coated polydimethylsiloxane (PDMS) substrata induced increased differentiation and decreased proliferation [4]. Furthermore, the interaction of the ECM ligand with the substratum material affects its adsorption or binding to the substratum material, which can in turn affect cell adhesion and subsequent cell responses [159–161].

4.1.4. Substratum stiffness and fiber geometry are the most studied mechanical cues

Below, we summarize the effect of substratum stiffness and fiber geometry on neural stem cells (NSC) and OPC.

When adult rat NSC were exposed to laminin-coated substrata of varying stiffness, the stiffer (1, 3.5 and 7 kPa) methylacrylamide chitosan substrata yielded a higher percentage of RIP + cells [141], while compliant (0.1, 1, 10 and 100 kPa) polyacrylamide substrata yield a higher percentage of MBP + cells [142]. For neonatal rat OPCs cultured on polyacrylamide substrata of varying stiffness, the percentage of MBP + cells decreased with increasing stiffness (30 kPa *vs*. 1.5 kPa) on Matrigel coating [9], but increased with increasing stiffness (70 kPa > 1 kPa > 0.7 kPa; and 0.4 kPa > 0.1 kPa) on PDL coating [5].

For electrospun fibers, geometric considerations have included fiber alignment and diameter. More NSC differentiated to OPCs when cultured on randomly distributed fibers than on aligned fibers [148]. As far as fiber diameter is concerned, more NSC differentiated into RIP + cells when cultured on electrospun polyethersulfone fibers of smaller diameter (283 nm *vs*. 749 nm) in the presence of retinoic acid [149]. On the other hand, OPC differentiation into MBP + cells was greater on polycaprolactone fibers of larger diameter (2 μm *vs*. 700 nm or 300 nm) coated with dihydroxy phenylalanine in the presence of miR-219/338 [153]. This observation of larger diameter favoring OPC differentiation toward mature OL was repeated over a similar range of fiber diameter (4 μm *vs*. 400 nm) and different composition (poly L-lactic acid) in quantification of MBP overlay suggestive of fiber wrapping [6].

4.1.5. Fewer studies on human OLs

Most mechanostimulation studies to date have been conducted with either murine NSC or murine OPC (of mouse or rat origin). While these studies have laid the groundwork showing the effect of mechanical cues on OPC biology, future mechanotransduction and mechanostimulation studies with human iPSC-derived neuroglia may potentially improve *in vitro* methods to generate human OPCs and oligodendrocytes.

4.2. Mechanotransduction

4.2.1. Generic mechanotransduction pathway in adherent cells

The typical pathway for mechanosensing and signal transduction [162–166] in adherent cells – including neuroglia such as OL – begins at the interaction between cell transmembrane receptors, called integrins, and extracellular ligand [167]. This bond is further linked from the cytosolic domain of integrins to the cytoskeleton *via* a group of adaptor and scaffolding proteins, called focal adhesions. Adherens junctions [168] (cell-cell junction) and stretch-activated ion channels [169] on the cell membrane act as additional routes for delivery of mechanical cues to the cell. Under mechanical force, integrins and focal adhesion proteins such as talin, vinculin, and p130cas change conformation, resulting in exposure of new binding sites and – for catch-bond interactions – can be strengthened under tensile force exerted by the cell itself or by an extracellular stimulus [170–174]. Next in the signaling cascade, several of the adaptor and scaffolding proteins at focal adhesions, such as Rho GTPases, focal adhesion kinases (FAK) and mitogen-activated protein kinases (MAPK), may be dynamically recruited, released or phosphorylated [175], [176]. These proteins from focal adhesion and calcium ions from stretch-activated ion channels, provide signals for remodeling of the cytoskeleton [177–180]. Cytoskeletal remodeling affects tension in the cytoskeleton and the orientation of cytoskeletal filaments, which in turn affect the magnitude and direction of force generated and transmitted by the cytoskeleton [181], [182]. The major source of force generation by the cytoskeleton are the myosin II−A and IIB− motors on actin [183]. In addition to force transmission, cytoskeleton remodeling plays a role in modulation of cytoplasmic *vs* nuclear localization of some transcription regulators such as yes associated protein (YAP) [184–186], megakaryoblastic leukemia (MKL) [187] and chromatin modification enzymes such as histone deacetlyases (HDACs) [188]. Next in the physical link, the cytoskeleton is tethered to the nucleus *via* the LINC (linker of nucleoskeleton and cytoskeleton) complex, comprising transmembrane proteins of the nuclear envelope like nesprin (on outer nuclear membrane) and emerin (on the inner nuclear membrane) [162], [189]. On the nucleoplasmic side, emerins and lamin B receptors bind to the lamin meshwork, which anchors the chromatin with help of several chromatin binding proteins [190]. While forces from the cytoskeleton can directly be transmitted *via* this physical link to chromatin, resulting in gene repositioning and chromosome reorganization, cytoskeletal forces can also activate mechanosensitive proteins in this physical link, starting another downstream signaling cascade [191].

4.2.2. Sensing strain, rigidity, and topography

Cells can sense extracellular strain, substratum rigidity, and topographical cues through this mechanosensing and signal transduction pathway. The immediate effects of extracellular strain are protein conformation changes, reinforcement of catch bonds, opening of stretch-activated ion channels, and chromatin reorganization *via* direct transmission of force *via* the physical link [192], [193]. On the other hand, substratum stiffness and topographical cues are first converted to force before engaging the mechanotransduction pathway. Substratum stiffness is sensed *via* a pulling force on the nascent focal adhesions at the cell leading edge, generated by the contractile actomyosin units within the cells [194], [195]. These contractile units feedback to the focal adhesion formation, which are either reinforced or suppressed depending on rigidity [196], [197]. Substratum topography (shape and dimension of physical features) affects the size, orientation, and distribution of focal adhesion formation, which in turn affects the strength and orientation of the cytoskeleton, thereby affecting the forces generated by the cytoskeleton [196–199]. Note that most of these observations have been made *in vitro* for cells adhered to materials of stiffness that is high relative to the CNS tissue and cells.

4.2.3. How mechanical cues mediate lineage-specificity

A few recent studies have shown the involvement of this generic pathway in OL mechanotransduction [3], [4], [7], [137], [143], [200]. However, it is not yet fully understood how this mechanotransduction response elicits transcription of myelin-specific genes, driving differentiation and myelination of OPC. Mechanical cue-mediated OL lineage

specificity and myelination can be achieved in three ways: *(1) Activation of lineage-specific transcription regulators:* For example, GATA4, activated by mechanical stretching of ventricles, is specific for cardiac development; RUNX2, phosphorylated by mechano-activated MAPK, regulates osteoblast-specific differentiation; and MEF2 and MYOD1, activated by calcineurin, a downstream target of load mediated calcium signaling, mediate myogenesis in skeletal muscle [201]. While the mechanosensitive transcription regulator YAP has been implicated in mechanoresponse of OL [4], [137], its known role in the nucleus is general activation of proliferation genes and suppression of apoptotic genes [202], [203]. How YAP mediates transcription of myelin-specific gene programs is still unclear. Olig-1, an OL specific transcription factor that facilitates MBP expression when it localizes in the nucleus, and facilitates membrane expansion when it localizes in the cytosol [204], [205], has been observed to exhibit higher nuclear levels in OPC on stiffer substrata (30 kPa compared to 1.5 kPa) [9]. However, it is still unclear whether extracellular stiffness directly affects intracellular Olig-1 localization directly or indirectly. *(2) Activation of lineage-specific chromatin modifiers:* There are examples of OL lineage-specific chromatin modifiers [206], [207]. However, to our knowledge there are currently no published examples of mechanically activated OL lineage-specific chromatin modifiers. Generic chromatin modification enzymes may be activated by mechanical cues; for example, HDAC3 is activated by specific cell geometry cues in fibroblasts [188]. Future experiments can consider mechanoresponsive OL-lineage-specific and myelination-specific chromatin modifiers from the list of OL lineage-specific chromatin modifiers [206], [207]. *(3) Lineage-specific changes in chromosome and gene positioning:* Recent studies in mechanobiology [208] [209], have shown the possibility of direct changes in chromosome organization by external mechanical cues *via* the actomyosin cytoskeleton, LINC complex and lamin network. This possibility could be further explored by tracking position and organization of myelin-specific genes or chromosomes *via* fluorescence *in situ* hybridization in mechanically stimulated cells.

5. Implications of OL mechanosensitivity for research and treatment of neurological diseases

We can now contemplate two important implications of OL mechanosensitivity. First, mechanical forces and changes in the OL environment may directly or indirectly regulate therapeutic efficacy of small molecules, antibodies, and exogenous cells *in vivo*. Second and distinctly, we may also harness these forces as engineering tools *in vitro* to improve the development and therapeutic effect of these treatments – including the availability of human cells for such studies.

5.1. Potential implications of mechanics in CNS pathology and therapeutic efficacy

The downstream effects of mechanical forces and changes, and dysregulation of mechanisms of mechanosensing, are difficult to estimate and may have important implications in the efficacy of drug and cell therapies [210]. Important lessons may be learned from oncology. The mechanical environment plays an important role in cancer progression (cell motility and growth kinetics) and drug resistance, and chemotherapeutics directly targeting mechanisms of sensing and adaptation have been developed [211–215]. A number of genetic and acquired CNS disorders are characterized by myelin irregularities and damage; OL death and dysfunction; and disturbance of the axon-glia complex [216]. Several small molecules have been proposed as promoters of OPC maturation and myelin repair in animal models: muscarinic receptor antagonists (clemastine, benzotropine, quetiapine, clobetasol, oxubutynin, trospium, ipratropium) [139], [217–219], cytochrome P450 inhibitors (miconazole, ketoconazole) [217], gamma-secretase inhibitors (DAPT, LY411,575, BMS708,163, MRK560) [220], kinase inhibitors (imatinib mesylate) [220], anti-cholinergics (atracurium besylate) [220], mitotic inhibitors (docetaxel) [220], ion channel blockers (zu-capsaicin, amiloride, Oxcarbazepine) [220] and ATPase inhibitors (digoxin) [220] and estrogen receptor modulators (bazedoxifene) [221]. Clemastine has further shown modest efficacy in a human clinical trial against chronic demyelinating optic neuropathy [222]. The mechanism of action in the OL machinery has only recently been partially elucidated for some of these repurposed drugs (cholesterol synthesis pathway [221] [223],). Given the mechanosensing capabilities of neuroglia and abundance of mechanosensing proteins in the CNS, it is not unexpected that mechanotransduction may play a role in these mechanisms. The MAPK pathway, which is activated by mechanical signals [224] and PIEZO channels [225] is involved in the remyelination mechanism of miconazole, a recently repurposed antifungal [217]. The differential expression of mechanosensing channels and receptors across disease, aging, and development also has important implications for CNS drug development. The process of aging not only affects cell and tissue mechanics, but also the ability of cells to sense changes in the mechanical landscape, and to transduce those changes into biological processes [226]. Pathological conditions can, for example, affect the mechanosensing capabilities of astrocytes by changing the expression of mechanosensing Piezo1 channels [227]. Mechanotransduction may itself be an important part of the pathology of CNS disorders. For example, tissue stiffness and mechanotransduction signaling are altered in Alexander's disease, one of the rare leukodystrophies [228]. This is at least one example where dysregulation of a mechanotransduction signaling cascade has been linked to behavioral dysfunction. Through understanding OL mechanotransduction we may elucidate biochemical handles to correct mechanics-mediated damage, and recapitulate mechanics-mediated biological processes that may help improve OPC differentiation into mature myelinating OL (oligodendrogenesis) and efficient myelination or remyelination *in vivo*.

5.2. Potential use of mechanical cues to address challenges in human oligodendrocyte generation

As we work toward resolving outstanding challenges in brain mechanobiology (namely, reconciling mechanical cues with cell response and function), we can leverage these findings to address technical challenges in CNS research and therapeutic development. CNS biomechanics and mechanotransduction may be used as tools to identify new avenues for therapeutic intervention, to enrich heterogeneous cell populations, to direct cell fates and scale-up cell production, and to develop better biomarkers. Three technologies have revolutionized neuroscience research in the last thirty years: (1) the induced pluripotency of human somatic cells [229], [230], (2) single-cell RNA (scRNA-seq) sequencing and bioinformatics [231], [232], and (3) genome editing *via* CRISPR and related approaches [233–235]. The discovery of human induced pluripotent stem cells (hiPSCs) has catalyzed the generation of human OLs [145], [236–246]. Combined with CRISPR genome editing, patient-specific disease models with isogenic (*i.e.*, from the same genotype) controls have been developed [247–249]. One of the outstanding challenges in hiPSC technology is the phenomenon of cell population heterogeneity. For systematically generated lines, heterogeneity or variability of hiPSC-derived cells arise primarily from the genetic variability across human populations, but also from the efficacy of downstream differentiation methods for even a single donor cell source [249]. Most chemical induction protocols for OL differentiation generate diverse populations of neuroglia cells, the composition of which depends at least on the type and timing of chemical patterning. HiPSC-derived OL cell enrichment using well-known surface antigens has been reported (A2B5 [236], [240], Sulfatide-recognizing O4 [218], [237], CD140a and CD9 [240]). However, as has been demonstrated previously and reinforced by scRNA-seq [250–255], few of these surface antigens and their encoding-genes are differentially expressed between neuroglia populations in the CNS. Furthermore, their expression may vary across human OL subtypes [256], [257], and

the *in vitro* viability of sorted cells is quite limited [237]. While the CD140a antigen recognizing the PDGF receptor alpha in OPCs has shown great promise for enrichment of hiPSC-derived OL precursors or hOPC [240], results have not yet been sufficiently reproduced nor tested with protocols that co-generate neurons and thus require further exploration.

Physical forces and mechanical cues may be harnessed to address population heterogeneity upstream by guiding lineage specification and progression, and downstream by facilitating label-free separation of key cell subpopulations such as OL. While scRNA-seq is a powerful tool for identification of novel surface markers with sufficient specificity to meet the current need, label-free separation approaches also offer unique opportunities that include potential universality across differentiation protocols, cheaper and faster methods, scalability with high level of parallelization, which may become important as we draw closer to personalized medicine, and yielding unlabeled cells closer to clinical compliance. Label-free methods have been optimized to separate primary cells from rat, mouse, and human brains [258–261]. While the same principles may be applicable to derived neuroglia, these have not yet been demonstrated, and few have been optimized to enrich for the oligodendrocyte population. More research is required to elucidate differences across various OL, astrocyte, and OL subtypes. Further mechanical characterization can also help reconcile physical and mechanical attributes (*e.g.*, differences in cell stiffness) with cell identity, and construct novel separation schemes based on biophysical attributes.

Challenges in downstream isolation of hiPSC-derived OL-lineage subpopulations of interest could be at least partially circumvented by improving protocol efficiency upstream. Direct and transcription factor-mediated OL differentiation protocols have been reported [157], [262], [263]. These promise higher cell type homogeneity, faster and scalable procedures. However, these methods have been less tested; the modifications therein yield cells that currently cannot be used in patients, and may bypass important maturation steps in the cells' development. Little is also known about the unintended changes that forced transcription factor overexpression may cause on the intended OL phenotype. Three-dimensional culture systems have been engineered to improve early hOPC differentiation [145]; reprogram somatic cells to pluripotency [264]; generate patterned tissues from pluripotent stem cells [265]; expand iPSCs [266] and drive the formation of human organoids [267–269]. Increasing insights into the complexity of OL mechanosensitivity and its manifestation in human cells will help shape new tools and approaches to further optimize oligodendrogenesis from hiPSCs.

5.3. Other uses of CNS mechanics as engineering and diagnostic tools

Additional challenges remain in hiPSC technology and CNS research and therapy, for which engineering approaches may be valuable. Functional maturity of hiPSC-derived OL may be critical to model and study the progression of human development and aging diseases such as Alzheimer's, Parkinson's and amyotrophic lateral sclerosis (ALS). While most hiPSC-derived CNS cells resemble fetal maturity, functional maturity has been achieved by long-term culture ($>$ 12 months). However, better modeling of the 3D physical and mechanical extracellular environment may accelerate or better recapitulate neuroglia maturation [270] [271], and promote higher yield and greater homogeneity of the cell population phenotype. Cell proliferation is also critical to achieve the cell numbers necessary for scale up and manufacturing [272], and cost-effective strategies will be necessary to realize the potential of such approaches for cell-based therapy. Various modalities of 3D culture have been adapted for expansion of embryonic, mesenchymal and induced pluripotent stem cells and derivatives [273]. Dynamic and static mechanical cues noted above in basic research studies of OL mechanical regulation may also be used to increase the rate and scale of proliferation of certain neuroglia lineages. Interesting and novel ideas such as simulated microgravity have also been pursued [274].

Changes in mechanical properties of tissue may also be harnessed to develop non-invasive biomarkers. The magnitude of tissue strain has been suggested as a discriminator between glioma and normal brain tissue [51], *in vivo* magnetic resonance elastography (MRE) measurements infer estimated tissue stiffness and correlate with intracranial pressure [275], [276], and water diffusion changes are common global markers for myelin content [277]. More sensitive and specific techniques are yet to be developed to capture de- and remyelination at the microscale *in vivo*.

6. Outstanding questions and future directions

Mechanobiology of the CNS is a relatively new field of exploration. Although the community has expanded our understanding of how neural cells including neuroglia and their progenitors respond to mechanical cues, many important questions remain unanswered. Next we consider a few of those outstanding questions that we feel should be addressed by further studies.

6.1. What magnitudes, exposure times, modes, and combination of cues are sufficient to induce significant changes of OPC biology?

Different mechanical cues can enhance or decrease processes such as OPC migration, proliferation, and differentiation. However, we do not know the threshold magnitudes of those various cues sufficient to induce measurable differences in these processes. These thresholds will likely be different for each process. For example, we observed an increasing trend in average MBP expression between OPC populations cultured on the range of substrata with stiffness from 0.1 to 1.0 kPa [5]. This trend however was non-linear; an increase observed between 0.1 and 0.4 kPa stiffness conditions was larger than the changes observed between 0.4 and 0.7 kPa. This suggests that in the tissue, stiffness changes within 0.4 and 0.7 kPa range may be less impactful for OPC differentiation than the changes from 0.4 to 0.1 kPa. In contrast, for OPC proliferation we observed no changes on gels with stiffness 0.1 and 0.4 kPa, but significant increase when stiffness increased to 0.7 kPa. Studies of strain effect on OPCs were conducted under static strains of 10–15 % [4], [7], which were sufficient to induce changes in OPC proliferation and differentiation. However, we do not know the minimum threshold of tensile strain that can cause observable changes in these processes. It is also not clear how temporal duration of these cues would affect OPC biology. For example, in our studies to assess the effect of substratum stiffness on OPC differentiation, the cells were grown on gels with defined stiffness for 3 days and after reaching this time in culture the MBP expression was measured by immunostaining [5]. While that experimental design demonstrated increased MBP expression on stiffer gels over the range considered, it is not known whether the increase in MBP expression would be still observed if cells were exposed to stiffer conditions for a shorter duration than 3 days, then transferred to a more compliant substratum and tested for MBP expression after reaching the day 3 time point. In our strain studies, tensile static strain was applied for 3 and 5 days [4]. Would shorter strain duration or dynamic strain modes be sufficient to trigger or increase OPC differentiation to the same extent? Do OPCs have stiffness and strain memory, before or even after cell doubling, due to epigenetic modifications? In other words, can mechanical cues trigger the process of differentiation, which then proceeds even when the cue is no longer present? Finally, various cues act on cells simultaneously *in vivo*. We do not know how combinations of different cues affect OPC biology. It is possible that some combination of these cues, with specific magnitudes and modes, can be synergistic or antagonistic.

6.2. Are mechanical cues that are accessible in vitro also meaningful in vivo?

Although separate mechanical cues studied *in vitro* can have

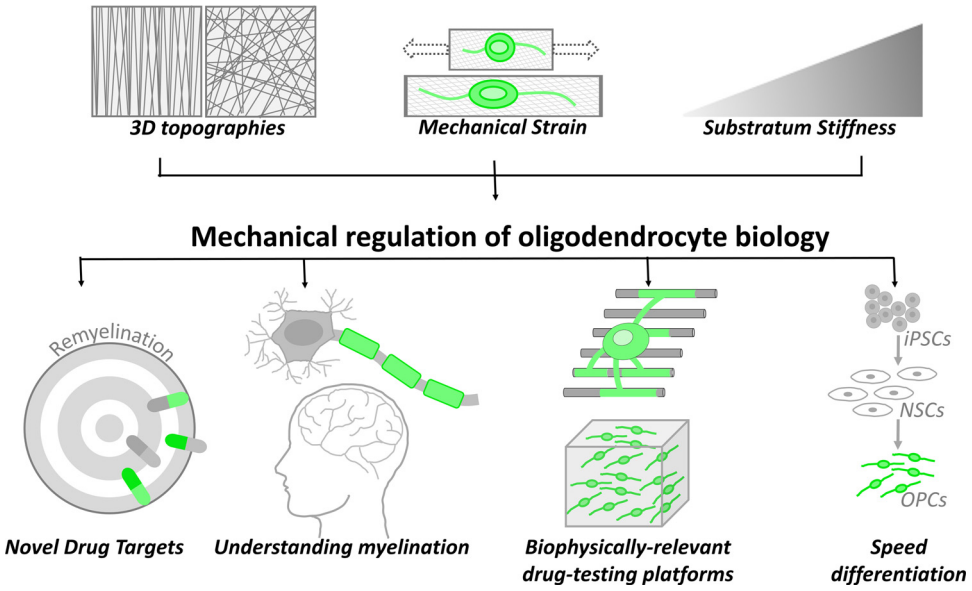

Fig. 3. Implications of oligodendrocyte mechanoregulation studies.
Mechanoregulation of oligodendrocyte biology *via* engineered mechanical cues *in vitro* has prospective applications in (1) discovering novel drug targets for myelination from mechanotransduction pathway; (2) understanding how *in vivo* mechanical environment affects myelination in health and disease; (3) using biophysically relevant platforms for drug testing; and (4) speeding the generation of human oligodendrocytes from human induced pluripotent stem cells.

significant observable effects on OPC biology, those cues are but a small fraction of all the cues that act on OPC concurrently *in vivo*. It is not clear which of the mechanical cues, and at what magnitudes, may be significant in the presence of biochemical factors. To address these questions, studies of more complex design are required. Further, such experiments should be designed and described to *either* recapitulate a mechanical cue that is present *in vivo* (*i.e.*, as a platform to learn about developmental or disease responses) or to manipulate mechanotransductive pathways as an intervention (*i.e.*, as a tool, in which case it is not necessary that the cue be present under physiological or pathological conditions *in vivo*) (Fig. 3).

6.3. What are the mechanotransduction mechanisms and involved signaling pathways for various mechanical cues?

More detailed understanding of the mechanisms governing mechanotransduction opens opportunities to develop therapeutic approached based on these mechanisms. The mechanisms of how strain and stiffness may increase OPC differentiation and formation of compact myelin sheaths in myelination or remyelination *in vivo* are not yet fully understood. Even if strain will not be applied to OPC *in vivo* to elicit differentiation and promote myelination, understanding the pathways by which strain promotes such a response can reveal drug target opportunities.

6.4. Are human OPCs also mechanosensitive?

Studies of mechanosensitivity have been limited to use of murine OPC for practical reasons related to human OPC availability and challenges in hiPSC-derived OPC generation and purification. Are human OPC similar in their responses to mechanical cues; are they mechanosensitive at all? Ultimately, we must understand mechanosensitivity of human OPCs to be able to use this knowledge for therapeutic advantage. The emerging access to OPC and OL of human origin provides a necessary component of answering these questions, and will require improved differentiation and purification of cell populations to ask these questions well. Indeed, it is possible but not yet established that mechanical cues (among others such as physical cues of synthetic matrices or substrata) can also help improve that yield of hiPSC-derived OPC and OL (Fig. 3).

6.5. Future directions in OPC mechanobiology

In continuation of efforts to understand mechanobiology of OL and other neuroglia, it will be essential to understand what types and magnitudes of distinct mechanical cues exist in the *in vivo* environment of the nervous system and how this mechanical environment changes in the disease. Development of materials that can match neural tissue and neural cell mechanical properties, as well as progress in generation of human neural cells and organoids from healthy and disease carrying donors, provides new means to build such *in vitro* models. These models can be also used to test how physiological and pathological mechanical cues affect different aspects of OL biology, including differentiation and myelin formation. Increasing access to human cells from both healthy and diseased donors opens now possibilities to model mechanical environment characteristic of specific diseases. Such models can be important tools to test cells responses to therapeutics in a disease context, for which the mechanical environment can and does differ from that of healthy tissue. Furthermore, development of the reductionist models of *in vitro* CNS environments will be essential to understand mechanotransduction and evaluate the impact of specific mechanical cues in the context of other factors.

Understanding when and how mechanical cues can promote OL differentiation and myelination could open new avenues for therapeutic applications (Fig. 3). For example, we could explore biomolecules emerging from mechanotransduction pathways as new targets for pharmacological compounds to stimulate myelin repair. Another potential area of application is improving the *in vitro* protocols of generation of human neuroglia from stem cells, by applying mechanical cues that accelerate differentiation into the desired lineage. Together, the biological and materials engineering approaches that allow us to probe and exploit mechanical regulation in OL differentiation and key functions such as myelination set the stage for an exciting decade of interdisciplinary discovery for both fundamental research and therapeutic applications.

Acknowledgements

This work was supported by grants from National Institutes of Health, USA under award number 5-R21-NS102762-02 and the National Research Foundation-Prime Minister's office, Republic of Singapore under its Campus for Research Excellence and Technological Enterprise (CREATE) program, through Singapore-MIT Alliance for Research and Technology Centre (SMART): BioSystems and

Micromechanics (BioSyM), and Critical Analytics for Manufacturing Personalized-Medicine (CAMP) Inter-Disciplinary Research Groups.

References

[1] M.E. Bechler, L. Byrne, C. Ffrench-Constant, CNS myelin sheath lengths are an intrinsic property of oligodendrocytes, Curr. Biol. 25 (September 18) (2015) 2411–2416.
[2] D. Espinosa-Hoyos, et al., Engineered 3D-printed artificial axons, Sci. Rep. 8 (December 1) (2018) 478.
[3] M. Hernandez, J. Patzig, S.R. Mayoral, K.D. Costa, J.R. Chan, P. Casaccia, Mechanostimulation promotes nuclear and epigenetic changes in oligodendrocytes, J. Neurosci. 36 (January 3) (2016) 806–813.
[4] A. Jagielska, et al., Mechanical strain promotes oligodendrocyte differentiation by global changes of gene expression, Front. Cell. Neurosci. 11 (2017) 93.
[5] A. Jagielska, A.L. Norman, G. Whyte, K.J. Van Vliet, J. Guck, R.J.M. Franklin, Mechanical environment modulates biological properties of oligodendrocyte progenitor cells, Stem Cells Dev. 21 (November 16) (2012) 2905–2914.
[6] S. Lee, et al., A culture system to study oligodendrocyte myelination processes using engineered nanofibers, Nat. Methods 9 (September 9) (2012) 917–922.
[7] E. Makhija, et al., Mechanical strain alters cellular and nuclear dynamics at early stages of oligodendrocyte differentiation, Front. Cell. Neurosci. 12 (March) (2018) 59.
[8] S.S. Rosenberg, E.E. Kelland, E. Tokar, A.R. De La Torre, J.R. Chan, The geometric and spatial constraints of the microenvironment induce oligodendrocyte differentiation, Proc. Natl. Acad. Sci. 105 (September 38) (2008) 14662–14667.
[9] M.M. Urbanski, et al., Myelinating glia differentiation is regulated by extracellular matrix elasticity, Sci. Rep. 6 (December 1) (2016) 33751.
[10] Y.K. Mariappan, K.J. Glaser, R.L. Ehman, Magnetic resonance elastography: a review, Clin. Anat. 23 (June 5) (2010) 497–511.
[11] E.P. Canovic, et al., Characterizing multiscale mechanical properties of brain tissue using atomic force microscopy, impact indentation, and rheometry, J. Vis. Exp. (115) (2016).
[12] M.R. VanLandingham, Review of instrumented indentation, J. Res. Inst. Stand. Technol. 108 (July 4) (2003) 249.
[13] A.S. Mijailovic, B. Qing, D. Fortunato, K.J. Van Vliet, Characterizing viscoelastic mechanical properties of highly compliant polymers and biological tissues using impact indentation, Acta Biomater. 71 (April) (2018) 388–397.
[14] S. Budday, G. Sommer, J. Haybaeck, P. Steinmann, G.A. Holzapfel, E. Kuhl, Rheological characterization of human brain tissue, Acta Biomater. 60 (September) (2017) 315–329.
[15] D.T.N. Chen, Q. Wen, P.A. Janmey, J.C. Crocker, A.G. Yodh, Rheology of Soft materials, Annu. Rev. Condens. Matter Phys. 1 (August 1) (2010) 301–322.
[16] N.I. Ozawa E, I. Nishino, Sarcolemmopathy: muscular dystrophies with cell membrane defects. - PubMed - NCBI, Brain Pathol. 11 (2001) 218–230.
[17] A. Gefen, S.S. Margulies, Are in vivo and in situ brain tissues mechanically similar? J. Biomech. 37 (September 9) (2004) 1339–1352.
[18] T.P. Prevost, A. Balakrishnan, S. Suresh, S. Socrate, Biomechanics of brain tissue, Acta Biomater. 7 (January 1) (2011) 83–95.
[19] F.B. Freimann, et al., Alteration of brain viscoelasticity after shunt treatment in normal pressure hydrocephalus, Neuroradiology 54 (March 3) (2012) 189–196.
[20] J. Guo, et al., Towards an elastographic atlas of brain anatomy, PLoS One 8 (August 8) (2013) e71807.
[21] M.C. Murphy, et al., Measuring the characteristic topography of brain stiffness with magnetic resonance elastography, PLoS One 8 (December 12) (2013) e81668.
[22] D.E. Koser, E. Moeendarbary, J. Hanne, S. Kuerten, K. Franze, CNS cell distribution and axon orientation determine local spinal cord mechanical properties, Biophys. J. 108 (May 9) (2015) 2137–2147.
[23] S. Budday, P. Steinmann, E. Kuhl, Physical biology of human brain development, Front. Cell. Neurosci. 9 (July) (2015) 257.
[24] N. Fattahi, et al., MR elastography demonstrates increased brain stiffness in normal pressure hydrocephalus, AJNR Am. J. Neuroradiol. 37 (March 3) (2016) 462–467.
[25] F. Dittmann, S. Hirsch, H. Tzschätzsch, J. Guo, J. Braun, I. Sack, In vivo wideband multifrequency MR elastography of the human brain and liver, Magn. Reson. Med. 76 (October 4) (2016) 1116–1126.
[26] D.E. Koser, et al., Mechanosensing is critical for axon growth in the developing brain, Nat. Neurosci. 19 (12) (2016) 1592–1598.
[27] C.A. Urbanczyk, M.L. Palmeri, C.R. Bass, Material characterization of in vivo and in vitro porcine brain using shear wave elasticity, Ultrasound Med. Biol. 41 (March 3) (2015) 713–723.
[28] S.A. Kruse, et al., Magnetic resonance elastography of the brain, Neuroimage 39 (January 1) (2008) 231–237.
[29] D.B. MacManus, B. Pierrat, J.G. Murphy, M.D. Gilchrist, Region and species dependent mechanical properties of adolescent and young adult brain tissue, Sci. Rep. 7 (December 1) (2017) 13729.
[30] A.E. Forte, S.M. Gentleman, D. Dini, On the characterization of the heterogeneous mechanical response of human brain tissue, Biomech. Model. Mechanobiol. 16 (no. 3) (2017) 907–920.
[31] E. Moeendarbary, et al., The soft mechanical signature of glial scars in the central nervous system, Nat. Commun. 8 (April 1) (2017) 14787.
[32] A.C. Pong, L. Jugé, L.E. Bilston, S. Cheng, Development of acute hydrocephalus does not change brain tissue mechanical properties in adult rats, but in juvenile rats, PLoS One 12 (August 8) (2017) e0182808.
[33] A.J. Thompson, I.K. Pillai, I.B. Dimov, C.E. Holt, K. Franze, Simultaneous in vivo time-lapse stiffness mapping and fluorescence imaging of developing tissue, bioRxiv (May) (2018) 323501.
[34] D. E. Koser, E. Moeendarbary, S. Kuerten, and K. Franze, Predicting local tissue mechanics using immunohistochemistry 1 2.
[35] D. Eberle, et al., Acute but not inherited demyelination in mouse models leads to brain tissue stiffness changes, bioRxiv (October) (2018) 449603.
[36] J. Vappou, E. Breton, P. Choquet, C. Goetz, R. Willinger, A. Constantinesco, Magnetic resonance elastography compared with rotational rheometry for in vitro brain tissue viscoelasticity measurement, Magn. Reson. Mater. Physics, Biol. Med. 20 (December 5–6) (2007) 273–278.
[37] U. Hamhaber, I. Sack, S. Papazoglou, J. Rump, D. Klatt, J. Braun, Three-dimensional analysis of shear wave propagation observed by in vivo magnetic resonance elastography of the brain, Acta Biomater. 3 (January 1) (2007) 127–137.
[38] D.I. Shreiber, H. Hao, R.A. Elias, Probing the influence of myelin and glia on the tensile properties of the spinal cord, Biomech. Model. Mechanobiol. 8 (August 4) (2009) 311–321.
[39] J.A.W. van Dommelen, T.P.J. van der Sande, M. Hrapko, G.W.M. Peters, Mechanical properties of brain tissue by indentation: interregional variation, J. Mech. Behav. Biomed. Mater. 3 (February 2) (2010) 158–166.
[40] A.F. Christ, et al., Mechanical difference between white and gray matter in the rat cerebellum measured by scanning force microscopy, J. Biomech. 43 (November 15) (2010) 2986–2992.
[41] F. Pervin, W.W. Chen, Effect of inter-species, gender, and breeding on the mechanical behavior of brain tissue, Neuroimage 54 (January) (2011) S98–S102.
[42] J. Zhang, M.A. Green, R. Sinkus, L.E. Bilston, Viscoelastic properties of human cerebellum using magnetic resonance elastography, J. Biomech. 44 (July 10) (2011) 1909–1913.
[43] S. Chatelin, A. Constantinesco, R. Willinger, Fifty years of brain tissue mechanical testing: from in vitro to in vivo investigations, Biorheology 47 (5–6) (2010) 255–276.
[44] S. Cheng, E.C. Clarke, L.E. Bilston, Rheological properties of the tissues of the central nervous system: a review, Med. Eng. Phys. 30 (December 10) (2008) 1318–1337.
[45] A. Gefen, N. Gefen, Q. Zhu, R. Raghupathi, S.S. Margulies, Age-dependent changes in material properties of the brain and braincase of the rat, J. Neurotrauma 20 (November 11) (2003) 1163–1177.
[46] K. Holtzmann, H.O.B. Gautier, A.F. Christ, J. Guck, R.T. Káradóttir, K. Franze, Brain tissue stiffness is a sensitive marker for acidosis, J. Neurosci. Methods 271 (2016) 50–54.
[47] J. Weickenmeier, M. Kurt, E. Ozkaya, M. Wintermark, K.B. Pauly, E. Kuhl, Magnetic resonance elastography of the brain: a comparison between pigs and humans, J. Mech. Behav. Biomed. Mater. 77 (January) (2018) 702–710.
[48] W. Zhang, et al., Effect of in vitro storage duration on measured mechanical properties of brain tissue, Sci. Rep. 8 (December 1) (2018) 1247.
[49] W. G. Bradley, A. R. Whittemore, A. S. Watanabe, S. J. Davis, L. M. Teresi, and M. Homyak, Association of deep white matter infarction with chronic communicating hydrocephalus: implications regarding the possible origin of normal-pressure hydrocephalus., AJNR. Am. J. Neuroradiol., vol. 12,1, pp. 31–39.
[50] M.L. Nogueira, J.V. Moreira, G.F. Baronzio, B. Dubois, J.-M. Steyaert, L. Schwartz, Mechanical stress as the common denominator between chronic inflammation, Cancer, and alzheimer's disease, Front. Oncol. 5 (2015).
[51] T. Selbekk, R. Brekken, O. Solheim, S. Lydersen, T.A.N. Hernes, G. Unsgaard, Tissue motion and strain in the human brain assessed by intraoperative ultrasound in glioma patients, Ultrasound Med. Biol. 36 (January 1) (2010) 2–10.
[52] Y.-B. Lu, et al., Viscoelastic properties of individual glial cells and neurons in the CNS, Proc. Natl. Acad. Sci. U. S. A. 103 (November 47) (2006) 17759–17764.
[53] S.W. Levison, J.E. Goldman, Both oligodendrocytes and astrocytes develop from progenitors in the subventricular zone of postnatal rat forebrain, Neuron 10 (February 2) (1993) 201–212.
[54] N.P. Pringle, W.D. Richardson, A singularity of PDGF alpha-receptor expression in the dorsoventral axis of the neural tube may define the origin of the oligodendrocyte lineage, Development 117 (February 2) (1993) 525–533.
[55] B.C. Warf, J. Fok-Seang, R.H. Miller, Evidence for the ventral origin of oligodendrocyte precursors in the rat spinal cord, J. Neurosci. 11 (August 8) (1991) 2477–2488.
[56] A.E. Warrington, E. Barbarese, S.E. Pfeiffer, Differential myelinogenic capacity of specific developmental stages of the oligodendrocyte lineage upon transplantation into hypomyelinating hosts, J. Neurosci. Res. 34 (January 1) (1993) 1–13.
[57] R.K. Small, P. Riddle, M. Noble, Evidence for migration of oligodendrocyte–type-2 astrocyte progenitor cells into the developing rat optic nerve, Nature 328 (July 6126) (1987) 155–157.
[58] R.J. Colello, M.E. Schwab, A role for oligodendrocytes in the stabilization of optic axon numbers, J. Neurosci. 14 (November 11 Pt 1) (1994) 6446–6452.
[59] B.P. Fulton, J.F. Burne, M.C. Raff, Visualization of O-2A progenitor cells in developing and adult rat optic nerve by quisqualate-stimulated cobalt uptake, J. Neurosci. 12 (12) (1992) 4816–4833.
[60] A. Gansmuller, E. Clerin, F. Kruger, M. Gumpel, F. Lachapelle, Tracing transplanted oligodendrocytes during migration and maturation in the Shiverer mouse brain, Glia 590 (1991).
[61] S. Nawaz, et al., Actin filament turnover drives leading edge growth during myelin sheath formation in the central nervous system, Dev. Cell 34 (July 2) (2015) 139–151.
[62] A. El Hady, B.B. Machta, Mechanical surface waves accompany action potential propagation, Nat. Commun. 6 (November 1) (2015) 6697.
[63] W.J. Tyler, The mechanobiology of brain function, Nat. Rev. Neurosci. 13

(December 12) (2012) 867–878.
[64] S.M. Corley, U. Ladiwala, A. Besson, V.W. Yong, Astrocytes attenuate oligodendrocyte death in vitro through an alpha(6) integrin-laminin-dependent mechanism, Glia 36 (December 3) (2001) 281–294.
[65] O. Schnädelbach, O.W. Blaschuk, M. Symonds, B.J. Gour, P. Doherty, J.W. Fawcett, N-cadherin influences migration of oligodendrocytes on astrocyte monolayers, Mol. Cell. Neurosci. 15 (March 3) (2000) 288–302.
[66] H.R. Payne, J.J. Hemperly, V. Lemmon, N-Cadherin expression and function in cultured oligodendrocytes, Dev. Brain Res. 97 (1996) 9–15.
[67] H. Kettenmann, B.R. Ranson, Electrical coupling between astrocytes and between oligodendrocytes studied in mammalian cell cultures, Glia 1 (January 1) (1988) 64–73.
[68] R. Bruzzone, T.W. White, D.A. Goodenough, The cellular internet: on-line with connexins, BioEssays 18 (September 9) (1996) 709–718.
[69] A. Battefeld, J. Klooster, M.H.P. Kole, Myelinating satellite oligodendrocytes are integrated in a glial syncytium constraining neuronal high-frequency activity, Nat. Commun. 7 (September 1) (2016) 11298.
[70] R.C. Pimentel, K.A. Yamada, A.G. Kléber, J.E. Saffitz, Autocrine regulation of myocyte Cx43 expression by VEGF, Circ. Res. 90 (April 6) (2002) 671–677.
[71] A. Salameh, K. Blanke, S. Dhein, Mind the gap! Connexins and pannexins in physiology, pharmacology and disease, Front. Pharmacol. 4 (2013) 144.
[72] C.P. Papaneophytou, et al., Regulatory role of oligodendrocyte gap junctions in inflammatory demyelination, Glia 66 (December 12) (2018) 2589–2603.
[73] J.L. Orthmann-Murphy, C.K. Abrams, S.S. Scherer, Gap junctions couple astrocytes and oligodendrocytes, J. Mol. Neurosci. 35 (May 1) (2008) 101–116.
[74] E. Syková, C. Nicholson, Diffusion in Brain Extracellular Space, Physiol. Rev. 88 (October 4) (2008) 1277–1340.
[75] Z. Wang, D.C. Thurmond, Mechanisms of biphasic insulin-granule exocytosis - roles of the cytoskeleton, small GTPases and SNARE proteins, J. Cell. Sci. 122 (April 7) (2009) 893–903.
[76] T. Grevesse, B.E. Dabiri, K.K. Parker, S. Gabriele, Opposite rheological properties of neuronal microcompartments predict axonal vulnerability in brain injury, Sci. Rep. 5 (August 1) (2015) 9475.
[77] A.M. Miller, N. Stella, Microglial cell migration stimulated by ATP and C5a involve distinct molecular mechanisms: quantification of migration by a novel near-infrared method, Glia 57 (June 8) (2009) 875–883.
[78] P. Moshayedi, et al., Mechanosensitivity of astrocytes on optimized polyacrylamide gels analyzed by quantitative morphometry, J. Phys. Condens. Matter 22 (May 19) (2010) 194114.
[79] P. Moshayedi, et al., The relationship between glial cell mechanosensitivity and foreign body reactions in the central nervous system, Biomaterials 35 (April 13) (2014) 3919–3925.
[80] L. Bollmann, et al., Microglia mechanics: immune activation alters traction forces and durotaxis, Front. Cell. Neurosci. 9 (September) (2015) 363.
[81] L. Chen, W. Li, V. Maybeck, A. Offenhäusser, H.J. Krause, Statistical study of biomechanics of living brain cells during growth and maturation on artificial substrates, Biomaterials 106 (2016) 240–249.
[82] F.X. Jiang, D.C. Lin, F. Horkay, N.A. Langrana, Probing mechanical adaptation of neurite outgrowth on a hydrogel material using atomic force microscopy, Ann. Biomed. Eng. 39 (2) (2013) 706–713.
[83] C.L. Wilson, L. Hayward, S. Kidambi, Advances Astrogliosis in a Dish : Substrate Stiffness Induces Astrogliosis in Primary Rat Astrocytes, (2016), pp. 34447–34457.
[84] H.H. Tsai, et al., Oligodendrocyte precursors migrate along vasculature in the developing nervous system, Science 351 (6271) (2016) 379–384.
[85] J. Villar, et al., WNT/β-catenin signaling is modulated by mechanical ventilation in an experimental model of acute lung injury, Intensive Care Med. 37 (July 7) (2011) 1201–1209.
[86] A. Goriely, et al., Mechanics of the brain: perspectives, challenges, and opportunities, Biomech. Model. Mechanobiol. 14 (October 5) (2015) 931–965.
[87] C.M. Dumont, et al., Factors released from endothelial cells exposed to flow impact adhesion, proliferation, and fate choice in the adult neural stem cell lineage, Stem Cells Dev. 26 (16) (2017) p. scd.2016.0350.
[88] W. Liu, et al., Perfusion deficits in patients with mild traumatic brain injury characterized by dynamic susceptibility contrast MRI, NMR Biomed. 26 (March 6) (2013) p. n/a-n/a.
[89] B. Beirowski, Concepts for regulation of axon integrity by enwrapping glia, Front. Cell. Neurosci. 7 (December) (2013) 256.
[90] C. Frühbeis, et al., Neurotransmitter-triggered transfer of exosomes mediates oligodendrocyte-neuron communication, PLoS Biol. 11 (July 7) (2013) e1001604.
[91] M. Bakhti, C. Winter, M. Simons, Inhibition of myelin membrane sheath formation by oligodendrocyte-derived exosome-like vesicles, J. Biol. Chem. 286 (1) (2011) 787–796.
[92] K. Franze, The mechanical control of nervous system development, Development 140 (August 15) (2013) 3069–3077.
[93] R. Sala-Llonch, D. Bartrés-Faz, C. Junqué, Reorganization of brain networks in aging: a review of functional connectivity studies, Front. Psychol. 6 (2015) 663.
[94] M. Morawski, M. Filippov, A. Tzinia, E. Tsilibary, L. Vargova, ECM in brain aging and dementia, Progress in Brain Research 214 (2014), pp. 207–227.
[95] A.I.M. Athamneh, D.M. Suter, Quantifying mechanical force in axonal growth and guidance, Front. Cell. Neurosci. 9 (2015) 359.
[96] S.M. Smith, et al., Correspondence of the brain's functional architecture during activation and rest, Proc. Natl. Acad. Sci. 106 (August 31) (2009) 13040–13045.
[97] P. Lamoureux, R.E. Buxbaum, S.R. Heidemann, Direct evidence that growth cones pull, Nature 340 (July 6229) (1989) 159–162.
[98] D.C. Van Essen, A tension-based theory of morphogenesis and compact wiring in the central nervous system, Nature 385 (January 6614) (1997) 313–318.
[99] M. Iwashita, N. Kataoka, K. Toida, Y. Kosodo, Systematic profiling of spatiotemporal tissue and cellular stiffness in the developing brain, Development 141 (October 19) (2014) 3793–3798.
[100] I. Sack, K.J. Streitberger, D. Krefting, F. Paul, J. Braun, The influence of physiological aging and atrophy on brain viscoelastic properties in humans, PLoS One 6 (9) (2011).
[101] A. Arani, et al., Measuring the effects of aging and sex on regional brain stiffness with MR elastography in healthy older adults, Neuroimage 111 (May) (2015) 59–64.
[102] M. Segel, et al., Niche stiffness underlies the ageing of central nervous system progenitor cells, Nature 573 (2019).
[103] L.M. Gerischer, et al., Combining viscoelasticity, diffusivity and volume of the hippocampus for the diagnosis of Alzheimer's disease based on magnetic resonance imaging, Neuroimage Clin. 18 (2018) 485–493.
[104] M.C. Murphy, et al., Regional brain stiffness changes across the Alzheimer's disease spectrum, Neuroimage Clin. 10 (2016) 283–290.
[105] M.C. Murphy, et al., Decreased brain stiffness in Alzheimer's disease determined by magnetic resonance elastography, J. Magn. Reson. Imaging 34 (September 3) (2011) 494–498.
[106] M.J. Menal, et al., Alzheimer's disease mutant mice exhibit reduced brain tissue stiffness compared to wild-type mice in both Normoxia and following intermittent hypoxia mimicking sleep apnea, Front. Neurol. 9 (January) (2018).
[107] K. Schregel, et al., Demyelination reduces brain parenchymal stiffness quantified in vivo by magnetic resonance elastography, Proc. Natl. Acad. Sci. 109 (April 17) (2012) 6650–6655.
[108] K. Riek, et al., NeuroImage: clinical Magnetic resonance elastography reveals altered brain viscoelasticity in experimental autoimmune encephalomyelitis, Neuroimage Clin. 1 (1) (2012) 81–90.
[109] M.M. Urbanski, M.B. Brendel, C.V. Melendez-Vasquez, Acute and chronic demyelinated CNS lesions exhibit opposite elastic properties, Sci. Rep. 9 (December 1) (2019) 999.
[110] K.-J. Streitberger, et al., Brain viscoelasticity alteration in chronic-progressive multiple sclerosis, PLoS One 7 (1) (2012) e29888.
[111] J. Wuerfel, et al., MR-elastography reveals degradation of tissue integrity in multiple sclerosis, Neuroimage 49 (February 3) (2010) 2520–2525.
[112] C. Klein, et al., Enhanced adult neurogenesis increases brain stiffness: in vivo magnetic resonance elastography in a mouse model of dopamine depletion, PLoS One 9 (3) (2014) e92582.
[113] A. Lipp, et al., Cerebral magnetic resonance elastography in supranuclear palsy and idiopathic Parkinson's disease, Neuroimage Clin. 3 (2013) 381–387.
[114] Y. Jamin, et al., Exploring the biomechanical properties of brain malignancies and their pathologic determinants in vivo with magnetic resonance elastography, Cancer Res. 75 (April 7) (2015) 1216–1224.
[115] K.M. Pepin, et al., MR elastography analysis of glioma stiffness and IDH1-Mutation status, AJNR Am. J. Neuroradiol. 39 (January 1) (2018) 31–36.
[116] D.C. Stewart, A. Rubiano, K. Dyson, C.S. Simmons, Mechanical characterization of human brain tumors from patients and comparison to potential surgical phantoms, PLoS One 12 (no. 6) (2017) 1–19.
[117] Z.S. Xu, et al., Evidence of changes in brain tissue stiffness after ischemic stroke derived from ultrasound-based elastography, J. Ultrasound Med. 32 (March 3) (2013) 485–494.
[118] A.R. Hackett, J.K. Lee, Understanding the NG2 glial scar after spinal cord injury, Front. Neurol. 7 (November) (2016) 1–10.
[119] J. Schaeffer, C. Cossetti, G. Mallucci, S. Pluchino, Multiple sclerosis, Neurobiology of Brain Disorders 1 Elsevier, 2015, pp. 497–520.
[120] F.B. Freimann, et al., MR elastography in a murine stroke model reveals correlation of macroscopic viscoelastic properties of the brain with neuronal density, NMR Biomed. 26 (November 11) (2013) 1534–1539.
[121] N. Antonovaite, S.V. Beekmans, E.M. Hol, W.J. Wadman, D. Iannuzzi, Regional variations in stiffness in live mouse brain tissue determined by depth-controlled indentation mapping, Sci. Rep. 8 (December 1) (2018) 12517.
[122] J. Weickenmeier, R. de Rooij, S. Budday, P. Steinmann, T.C. Ovaert, E. Kuhl, Brain stiffness increases with myelin content, Acta Biomater. 42 (2016) 265–272.
[123] J. Kwon, et al., Label-free nanoscale optical metrology on myelinated axons in vivo, Nat. Commun. 8 (1) (2017) 1–9.
[124] J. Ji, et al., Mitochondrial injury after mechanical stretch of cortical neurons in vitro: biomarkers of apoptosis and selective peroxidation of anionic phospholipids, J. Neurotrauma 29 (March 5) (2012) 776–788.
[125] A.C. Bain, D.F. Meaney, Tissue-Level Thresholds for Axonal Damage in an Experimental Model of Central Nervous System White Matter Injury, J. Biomech. Eng. 122 (6) (2000) 615.
[126] T.A. Gennarelli, et al., Axonal injury in the optic nerve: a model simulating diffuse axonal injury in the brain, J. Neurosurg. 71 (1989) 244–253.
[127] H. Hao, D.I. Shreiber, Axon kinematics change during growth and development, J. Biomech. Eng. 129 (August 4) (2007) 511.
[128] A.C. Bain, D.I. Shreiber, D.F. Meaney, Modeling of microstructural kinematics during simple elongation of central nervous system tissue, Trans. ASME 125 (December) (2003).
[129] S. Singh, A. A. Pelegri, David, and I. Shreiber, Characterization of the three-dimensional kinematic behavior of axons in central nervous system white matter, Biomech. Model. Mechanobiol.
[130] A. Breig, Biomechanics of the Central Nervous System: Some Basic Normal and Pathologic Phenomena, (1960).
[131] M.D. Tang-Schomer, A.R. Patel, P.W. Baas, D.H. Smith, Mechanical breaking of microtubules in axons during dynamic stretch injury underlies delayed elasticity, microtubule disassembly, and axon degeneration, FASEB J. 24 (May 5) (2010)

1401–1410.
[132] Y. Li, et al., Nanofibers support oligodendrocyte precursor cell growth and function as a neuron-free model for myelination study, Biomacromolecules 15 (January 1) (2014) 319–326.
[133] J.R. Tse, A.J. Engler, Stiffness gradients mimicking in vivo tissue variation regulate mesenchymal stem cell fate, PLoS One 6 (January 1) (2011) e15978.
[134] T. Betz, D. Koch, Y.-B. Lu, K. Franze, J.A. Käs, Growth cones as soft and weak force generators, Proc. Natl. Acad. Sci. U. S. A. 108 (August 33) (2011) 13420–13425.
[135] E. Fisher, et al., Imaging correlates of axonal swelling in chronic multiple sclerosis brains, Ann. Neurol. 62 (September 3) (2007) 219–228.
[136] A.S. Zeiger, et al., Static mechanical strain induces capillary endothelial cell cycle re-entry and sprouting, Phys. Biol. 13 (4) (2016) 046006.
[137] T. Shimizu, et al., YAP functions as a mechanotransducer in oligodendrocyte morphogenesis and maturation, Glia 65 (February 2) (2017) 360–374.
[138] A.A. Jarjour, H. Zhang, N. Bauer, C. ffrench-Constant, A. Williams, In vitro modeling of central nervous system myelination and remyelination, Glia 60 (January 1) (2012) 1–12.
[139] F. Mei, et al., Micropillar arrays as a high-throughput screening platform for therapeutics in multiple sclerosis, Nat. Med. 20 (October 2013) (2014) 954–960.
[140] M.E. Bechler, A neuron-Free microfiber assay to assess myelin sheath formation, Methods in Molecular Biology (Clifton, N.J.) 1936 (2019), pp. 97–110.
[141] N.D. Leipzig, M.S. Shoichet, The effect of substrate stiffness on adult neural stem cell behavior, Biomaterials 30 (December 36) (2009) 6867–6878.
[142] A.J. Keung, E.M. De Juan-Pardo, D.V. Schaffer, S. Kumar, TISSUE-SPECIFIC STEM CELLS Rho GTPases Mediate the Mechanosensitive Lineage Commitment of Neural Stem Cells, Stem Cells 29 (2011) 1886–1897.
[143] T. Lourenço, et al., Modulation of oligodendrocyte differentiation and maturation by combined biochemical and mechanical cues, Sci. Rep. 6 (April 1) (2016) 21563.
[144] C.R. Kothapalli, R.D. Kamm, 3D matrix microenvironment for targeted differentiation of embryonic stem cells into neural and glial lineages, Biomaterials 34 (August 25) (2013) 5995–6007.
[145] G.M.C. Rodrigues, et al., Defined and scalable differentiation of human oligodendrocyte precursors from pluripotent stem cells in a 3D culture system, Stem Cell Reports 8 (June 6) (2017) 1770–1783.
[146] S. Ankam, et al., Substrate topography and size determine the fate of human embryonic stem cells to neuronal or glial lineage, Acta Biomater. 9 (January 1) (2013) 4535–4545.
[147] H. Davis, X. Guo, S. Lambert, M. Stancescu, J.J. Hickman, Small molecule induction of human umbilical stem cells into myelin basic protein positive oligodendrocytes in a defined three-dimensional environment, ACS Chem. Neurosci. 3 (January 1) (2012) 31–39.
[148] M.K. Horne, D.R. Nisbet, J.S. Forsythe, C.L. Parish, Three-dimensional nanofibrous scaffolds incorporating immobilized BDNF promote proliferation and differentiation of cortical neural stem cells, Stem Cells Dev. 19 (June 6) (2010) 843–852.
[149] G.T. Christopherson, H. Song, H.-Q. Mao, The influence of fiber diameter of electrospun substrates on neural stem cell differentiation and proliferation, Biomaterials 30 (February 4) (2009) 556–564.
[150] J. Arulmoli, et al., Static stretch affects neural stem cell differentiation in an extracellular matrix-dependent manner, Sci. Rep. 5 (July 1) (2015) 8499.
[151] S. Shah, P.T. Yin, T.M. Uehara, S.-T.D. Chueng, L. Yang, K.-B. Lee, Guiding stem cell differentiation into oligodendrocytes using graphene-nanofiber hybrid scaffolds, Adv. Mater. 26 (June 22) (2014) 3673–3680.
[152] K. Yang, et al., Multiscale, hierarchically patterned topography for directing human neural stem cells into functional neurons, ACS Nano 8 (August 8) (2014) 7809–7822.
[153] H.J. Diao, W.C. Low, Q.R. Lu, S.Y. Chew, Topographical effects on fiber-mediated microRNA delivery to control oligodendroglial precursor cells development, Biomaterials 70 (November) (2015) 105–114.
[154] M.N. Asmani, et al., Three-dimensional culture of differentiated endometrial stromal cells to oligodendrocyte progenitor cells (OPCs) in fibrin hydrogel, Cell Biol. Int. 37 (December 12) (2013) 1340–1349.
[155] J.M. Maloney, E.B. Walton, C.M. Bruce, K.J. Van Vliet, Influence of finite thickness and stiffness on cellular adhesion-induced deformation of compliant substrata, Phys. Rev. E 78 (October 4) (2008) 041923.
[156] E.J. COLLARINI, et al., Growth factors and transcription factors in oligodendrocyte development, J. Cell. Sci. 1991 (February Supplement 15) (1991) 117–123.
[157] J. Wang, S.U. Pol, A.K. Haberman, C. Wang, M.A. O'Bara, F.J. Sim, Transcription factor induction of human oligodendrocyte progenitor fate and differentiation, Proc. Natl. Acad. Sci. 111 (July 28) (2014) E2885–E2894.
[158] B. Emery, Regulation of oligodendrocyte differentiation and myelination, Science (80-.) 330 (November 6005) (2010) 779–782.
[159] T. Razafiarison, et al., Biomaterial surface energy-driven ligand assembly strongly regulates stem cell mechanosensitivity and fate on very soft substrates, Proc. Natl. Acad. Sci. U. S. A. 115 (May 18) (2018) 4631–4636.
[160] V. Gribova, R. Auzely-Velty, C. Picart, Polyelectrolyte multilayer assemblies on materials surfaces: from cell adhesion to tissue engineering, Chem. Mater. 24 (March 5) (2012) 854–869.
[161] R.J. Wade, J.A. Burdick, Engineering ECM signals into biomaterials, Mater. Today 15 (October 10) (2012) 454–459.
[162] G.V. Shivashankar, Mechanosignaling to the cell nucleus and gene regulation, Annu. Rev. Biophys. 40 (June 1) (2011) 361–378.
[163] A.W. Orr, B.P. Helmke, B.R. Blackman, M.A. Schwartz, Mechanisms of Mechanotransduction, Dev. Cell 10 (January 1) (2006) 11–20.
[164] G. Charras, A.S. Yap, Tensile Forces and Mechanotransduction at Cell-Cell Junctions, Curr. Biol. 28 (April 8) (2018) R445–R457.
[165] N. Wang, Review of cellular mechanotransduction, J. Phys. D Appl. Phys. 50 (June 23) (2017).
[166] V. Vogel, M. Sheetz, Local force and geometry sensing regulate cell functions, Nat. Rev. Mol. Cell Biol. 7 (April 4) (2006) 265–275.
[167] Y. Chen, L. Ju, M. Rushdi, C. Ge, C. Zhu, Receptor-mediated cell mechanosensing, Mol. Biol. Cell 28 (November 23) (2017) 3134–3155.
[168] B. Ladoux, W.J. Nelson, J. Yan, R.M. Mège, The mechanotransduction machinery at work at *adherens* junctions, Integr. Biol. 7 (October 10) (2015) 1109–1119.
[169] B. Martinac, Mechanosensitive ion channels: molecules of mechanotransduction, J. Cell. Sci. 117 (May 12) (2004) 2449–2460.
[170] D.L. Huang, N.A. Bax, C.D. Buckley, W.I. Weis, A.R. Dunn, Vinculin forms a directionally asymmetric catch bond with F-actin, Science (80-.) 357 (August 6352) (2017) 703–706.
[171] Z. Sun, S.S. Guo, R. Fässler, Integrin-mediated mechanotransduction, J. Cell Biol. 215 (November 4) (2016) 445–456.
[172] M.A. Arnaout, S. Goodman, J.-P. Xiong, Structure and mechanics of integrin-based cell adhesion, Curr. Opin. Cell Biol. 19 (October 5) (2007) 495.
[173] E. Puklin-Faucher, M.P. Sheetz, The mechanical integrin cycle, J. Cell. Sci. 122 (January Pt 2) (2009) 179–186.
[174] Z. Sun, M. Costell, R. Fässler, Integrin activation by talin, kindlin and mechanical forces, Nat. Cell Biol. 21 (January 1) (2019) 25–31.
[175] P.P. Provenzano, P.J. Keely, Mechanical signaling through the cytoskeleton regulates cell proliferation by coordinated focal adhesion and Rho GTPase signaling, J. Cell. Sci. 124 (April Pt 8) (2011) 1195–1205.
[176] S. Huveneers, E.H.J. Danen, Adhesion signaling – crosstalk between integrins, Src and Rho, J. Cell. Sci. 122 (April 8) (2009) 1059–1069.
[177] J.L. Hoon, M.H. Tan, C.-G. Koh, The regulation of cellular responses to mechanical cues by rho GTPases, Cells 5 (April 2) (2016).
[178] N.O. Deakin, C.E. Turner, Paxillin comes of age, J. Cell. Sci. 121 (August 15) (2008) 2435–2444.
[179] F.-C. Tsai, G.-H. Kuo, S.-W. Chang, P.-J. Tsai, Ca2+ signaling in cytoskeletal reorganization, cell migration, and cancer metastasis, Biomed Res. Int. 2015 (April) (2015) 409245.
[180] P.K. Hepler, The cytoskeleton and its regulation by calcium and protons, Plant Physiol. 170 (January 1) (2016) 3–22.
[181] F.J. Alenghat, D.E. Ingber, Mechanotransduction: all signals point to cytoskeleton, matrix, and integrins, Sci. STKE 2002 (February 119) (2002) pe6.
[182] F. Martino, A.R. Perestrelo, V. Vinarský, S. Pagliari, G. Forte, Cellular mechanotransduction: from tension to function, Front. Physiol. 9 (July) (2018) 824.
[183] M.J. Greenberg, G. Arpağ, E. Tüzel, E.M. Ostap, A perspective on the role of Myosins as mechanosensors, Biophys. J. 110 (June 12) (2016) 2568–2576.
[184] J. Seo, J. Kim, Regulation of Hippo signaling by actin remodeling, BMB Rep. 51 (March 3) (2018) 151–156.
[185] O. Dobrokhotov, M. Samsonov, M. Sokabe, H. Hirata, Mechanoregulation and pathology of YAP/TAZ via Hippo and non-Hippo mechanisms, Clin. Transl. Med. 7 (August 1) (2018) 23.
[186] M. Kofler, P. Speight, D. Little, C. Di Ciano-Oliveira, K. Szászi, A. Kapus, Mediated nuclear import and export of TAZ and the underlying molecular requirements, Nat. Commun. 9 (December 1) (2018) 4966.
[187] H. Hirano, Y. Matsuura, Sensing actin dynamics: structural basis for G-actin-sensitive nuclear import of MAL, Biochem. Biophys. Res. Commun. 414 (October 2) (2011) 373–378.
[188] N. Jain, K.V. Iyer, A. Kumar, G.V. Shivashankar, Cell geometric constraints induce modular gene-expression patterns via redistribution of HDAC3 regulated by actomyosin contractility, Proc. Natl. Acad. Sci. U. S. A. 110 (July 28) (2013) 11349–11354.
[189] D.M. Graham, K. Burridge, Mechanotransduction and nuclear function, Curr. Opin. Cell Biol. 40 (2016) 98–105.
[190] T. Dechat, S.A. Adam, R.D. Goldman, Nuclear lamins and chromatin: when structure meets function, Adv. Enzyme Regul. 49 (1) (2009) 157–166.
[191] C. Uhler, G.V. Shivashankar, Regulation of genome organization and gene expression by nuclear mechanotransduction, Nat. Rev. Mol. Cell Biol. 18 (December 12) (2017) 717–727.
[192] R. De, A. Zemel, S.A. Safran, Do cells sense stress or strain? Measurement of cellular orientation can provide a clue, Biophys. J. 94 (March 5) (2008) L29–31.
[193] E.C. Yusko, C.L. Asbury, Force is a signal that cells cannot ignore, Mol. Biol. Cell 25 (November 23) (2014) 3717–3725.
[194] A.K. Yip, et al., Cellular response to substrate rigidity is governed by either stress or strain, Biophysj 104 (2013) 19–29.
[195] R. Bruinsma, Theory of force regulation by nascent adhesion sites, Biophys. J. 89 (July 1) (2005) 87–94.
[196] H. Wolfenson, et al., Tropomyosin controls sarcomere-like contractions for rigidity sensing and suppressing growth on soft matrices, Nat. Cell Biol. 18 (January 1) (2016) 33–42.
[197] G. Meacci, et al., α-Actinin links extracellular matrix rigidity-sensing contractile units with periodic cell-edge retractions, Mol. Biol. Cell 27 (22) (2016) 3471–3479.
[198] D.-H. Kim, P.P. Provenzano, C.L. Smith, A. Levchenko, Matrix nanotopography as a regulator of cell function, J. Cell Biol. 197 (April 3) (2012) 351–360.
[199] D. Hoffman-Kim, J.A. Mitchel, R.V. Bellamkonda, Topography, cell response, and nerve regeneration, Annu. Rev. Biomed. Eng. 12 (August) (2010) 203–231.
[200] R.W. O'Meara, J.-P. Michalski, R. Kothary, Integrin signaling in oligodendrocytes and its importance in CNS myelination, J. Signal Transduct. 2011 (December) (2011) 354091.
[201] A. Mammoto, T. Mammoto, D.E. Ingber, Mechanosensitive mechanisms in transcriptional regulation, J. Cell. Sci. 125 (July 13) (2012) 3061–3073.
[202] Z. Mohri, A. Del Rio Hernandez, R. Krams, The emerging role of YAP/TAZ in

mechanotransduction, J. Thorac. Dis. 9 (May. 5) (2017) E507–E509.
[203] B.C. Low, C.Q. Pan, G.V. Shivashankar, A. Bershadsky, M. Sudol, M. Sheetz, YAP/TAZ as mechanosensors and mechanotransducers in regulating organ size and tumor growth, FEBS Lett. 588 (August 16) (2014) 2663–2670.
[204] J. Dai, K.K. Bercury, W. Jin, W.B. Macklin, Olig1 Acetylation and Nuclear Export Mediate Oligodendrocyte Development, (2015).
[205] J. Niu, et al., Phosphorylated olig1 localizes to the cytosol of oligodendrocytes and promotes membrane expansion and maturation, Glia 60 (September 9) (2012) 1427–1436.
[206] J. Liu, P. Casaccia, Epigenetic regulation of oligodendrocyte identity, Trends Neurosci. 33 (April 4) (2010) 193–201.
[207] Y. Yu, et al., Olig2 targets chromatin remodelers to enhancers to initiate oligodendrocyte differentiation, Cell 152 (January 1–2) (2013) 248–261.
[208] Y.-C. Poh, et al., Dynamic force-induced direct dissociation of protein complexes in a nuclear body in living cells, Nat. Commun. 3 (January 1) (2012) 866.
[209] A. Tajik, et al., Transcription upregulation via force-induced direct stretching of chromatin, Nat. Mater. 15 (no. 12) (2016) 1287–1296.
[210] D.E. Ingber, I.I. Tensegrity, How structural networks influence cellular information processing networks, J. Cell. Sci. 116 (April 8) (2003) 1397–1408.
[211] J.-W. Shin, D.J. Mooney, Extracellular matrix stiffness causes systematic variations in proliferation and chemosensitivity in myeloid leukemias, Proc. Natl. Acad. Sci. 113 (October 43) (2016) 12126–12131.
[212] H.-H. Lin, et al., Mechanical phenotype of cancer cells: cell softening and loss of stiffness sensing, Oncotarget 6 (August 25) (2015) 20946–20958.
[213] T.A. Ulrich, E.M. de Juan Pardo, S. Kumar, The mechanical rigidity of the extracellular matrix regulates the structure, motility, and proliferation of glioma cells, Cancer Res. 69 (May 10) (2009) 4167–4174.
[214] S. Zustiak, R. Nossal, D.L. Sackett, Multiwell stiffness assay for the study of cell responsiveness to cytotoxic drugs, Biotechnol. Bioeng. 111 (February 2) (2014) 396–403.
[215] D.A. Reardon, L.B. Nabors, R. Stupp, T. Mikkelsen, Cilengitide: an integrin-targeting arginine-glycine-aspartic acid peptide with promising activity for glioblastoma multiforme, Expert Opin. Investig. Drugs 17 (8) (2010) 1225–1235.
[216] I.D. Duncan, A.B. Radcliff, Inherited and acquired disorders of myelin: the underlying myelin pathology, Exp. Neurol. 283 (September Pt B) (2016) 452–475.
[217] F.J. Najm, et al., Drug-based modulation of endogenous stem cells promotes functional remyelination in vivo, Nature 522 (June 7555) (2015) 216–220.
[218] M. Ehrlich, et al., Rapid and efficient generation of oligodendrocytes from human induced pluripotent stem cells using transcription factors, Proc. Natl. Acad. Sci. U. S. A. 114 (March 11) (2017) E2243–E2252.
[219] V.A. Deshmukh, et al., A regenerative approach to the treatment of multiple sclerosis, Nature 502 (7471) (2013) 327–332.
[220] K.D. Lariosa-Willingham, E.S. Rosler, J.S. Tung, J.C. Dugas, T.L. Collins, D. Leonoudakis, Development of a central nervous system axonal myelination assay for high throughput screening, BMC Neurosci. 17 (December 1) (2016) 16.
[221] K.A. Rankin, et al., Selective estrogen receptor modulators enhance CNS remyelination independent of estrogen receptors, J. Neurosci. 39 (March 12) (2019) 2184–2194.
[222] A.J. Green, et al., Clemastine fumarate as a remyelinating therapy for multiple sclerosis (ReBUILD): a randomised, controlled, double-blind, crossover trial, Lancet 390 (December 10111) (2017) 2481–2489.
[223] Z. Hubler, et al., Accumulation of 8,9-unsaturated sterols drives oligodendrocyte formation and remyelination, Nature 560 (August 7718) (2018) 372–376.
[224] L. Hoffman, C.C. Jensen, M. Yoshigi, M. Beckerle, Mechanical signals activate p38 MAPK pathway-dependent reinforcement of actin via mechanosensitive HspB1, Mol. Biol. Cell 28 (October 20) (2017) 2661–2675.
[225] A. Sugimoto, et al., Piezo type mechanosensitive ion channel component 1 functions as a regulator of the cell fate determination of mesenchymal stem cells, Sci. Rep. 7 (December 1) (2017) 17696.
[226] J.M. Phillip, I. Aifuwa, J. Walston, D. Wirtz, The mechanobiology of aging, Annu. Rev. Biomed. Eng. 17 (December 1) (2015) 113–141.
[227] M. Velasco-Estevez, et al., Infection augments expression of mechanosensing Piezo1 channels in amyloid plaque-reactive astrocytes, Front. Aging Neurosci. 10 (2018) 332.
[228] L. Wang, et al., Tissue and cellular rigidity and mechanosensitive signaling activation in Alexander disease, Nat. Commun. 9 (December 1) (2018) 1899.
[229] J. Yu, et al., Induced pluripotent stem cell lines derived from human somatic cells, Science (80-.) 318 (December 5858) (2007) 1917–1920.
[230] K. Takahashi, et al., Induction of pluripotent stem cells from adult human fibroblasts by defined factors, Cell 131 (November 5) (2007) 861–872.
[231] F. Tang, et al., mRNA-Seq whole-transcriptome analysis of a single cell, Nat. Methods 6 (May 5) (2009) 377–382.
[232] A.A. Kolodziejczyk, J.K. Kim, V. Svensson, J.C. Marioni, S.A. Teichmann, The technology and biology of single-cell RNA sequencing, Mol. Cell 58 (May 4) (2015) 610–620.
[233] L. Cong, et al., Multiplex genome engineering using CRISPR/Cas systems, Science (80-.) 339 (February 6121) (2013) 819–823.
[234] P. Mali, et al., RNA-guided human genome engineering via Cas9, Science (80-.) 339 (February 6121) (2013) 823–826.
[235] J.A. Doudna, E. Charpentier, The new frontier of genome engineering with CRISPR-Cas9, Science (80-.) 346 (November 6213) (2014) 1258096.
[236] S. Ogawa, Y. Tokumoto, J. Miyake, T. Nagamune, Induction of oligodendrocyte differentiation from adult human fibroblast-derived induced pluripotent stem cells, Vitr. Cell. Dev. Biol. - Anim. 47 (August 7) (2011) 464–469.
[237] P. Douvaras, V. Fossati, Generation and isolation of oligodendrocyte progenitor cells from human pluripotent stem cells, Nat. Protoc. 10 (August 8) (2015) 1143–1154.
[238] S.R.L. Stacpoole, et al., High yields of oligodendrocyte lineage cells from human embryonic stem cells at physiological oxygen tensions for evaluation of translational biology, Stem Cell Reports 1 (5) (2013) 437–450.
[239] A. Thiruvalluvan, et al., Survival and functionality of human induced pluripotent stem cell-derived oligodendrocytes in a nonhuman primate model for multiple sclerosis, Stem Cells Transl. Med. 5 (Novembe 11) (2016) 1550–1561.
[240] S. Wang, et al., Human iPSC-Derived oligodendrocyte progenitor cells can myelinate and rescue a mouse model of congenital hypomyelination, Cell Stem Cell 12 (February 2) (2013) 252–264.
[241] D.-S. Kim, et al., Rapid generation of OPC-like cells from human pluripotent stem cells for treating spinal cord injury, Exp. Mol. Med. 49 (July 7) (2017) e361.
[242] Y. Numasawa-Kuroiwa, et al., Involvement of ER stress in dysmyelination of pelizaeus-merzbacher disease with PLP1 missense mutations shown by iPSC-Derived oligodendrocytes, Stem Cell Reports 2 (May 5) (2014) 648–661.
[243] V. Meneghini, et al., Generation of human induced pluripotent stem cell-derived bona fide neural stem cells for ex vivo gene therapy of metachromatic leukodystrophy, Stem Cells Transl. Med. 6 (2) (2017) 352–368.
[244] D. Umebayashi, B. Coles, D. van der Kooy, Enrichment of oligodendrocyte progenitors from differentiated neural precursors by clonal sphere preparations, Stem Cells Dev. 25 (May 9) (2016) 712–728.
[245] M.R. Livesey, et al., Maturation and electrophysiological properties of human pluripotent stem cell-derived oligodendrocytes, Stem Cells 34 (April 4) (2016) 1040–1053.
[246] T. Yamashita, et al., Differentiation of oligodendrocyte progenitor cells from dissociated monolayer and feeder-free cultured pluripotent stem cells, PLoS One 12 (February 2) (2017) e0171947.
[247] M.S. Elitt, et al., Therapeutic suppression of proteolipid protein rescues Pelizaeus-Merzbacher disease in mice, bioRxiv (December) (2018) 508192.
[248] L.T. Ghaffari, A. Starr, A.T. Nelson, R. Sattler, Representing diversity in the dish: using patient-derived in vitro models to recreate the heterogeneity of neurological disease, Front. Neurosci. 12 (February) (2018) 1–18.
[249] B.J. Berry, S.T. Smith, E. Young, L. Mack, Advances and current challenges associated with the use of human induced pluripotent stem cells in modeling neurodegenerative disease, Cells Tissues Organs 98104 (2018) 331–349.
[250] H.S. Leong, et al., A global non-coding RNA system modulates fission yeast protein levels in response to stress, Nat. Commun. 5 (May) (2014) 3947.
[251] A.M. Falcão, et al., Disease-specific oligodendrocyte lineage cells arise in multiple sclerosis, Nat. Med. 24 (Decembet 12) (2018) 1837–1844.
[252] J. Newville, L.L. Jantzie, L.A. Cunningham, Embracing oligodendrocyte diversity in the context of perinatal injury, Neural Regen. Res. 12 (October 10) (2017) 1575–1585.
[253] B. Artegiani, A. Lyubimova, M. Muraro, J.H. Van Es, A. Van Oudenaarden, A single-cell RNA sequencing study reveals cellular and molecular dynamics of the hippocampal neurogenic niche, Cell Rep. 21 (2017) 3271–3284.
[254] D. van Bruggen, E. Agirre, G. Castelo-Branco, Single-cell transcriptomic analysis of oligodendrocyte lineage cells, Curr. Opin. Neurobiol. 47 (December) (2017) 168–175.
[255] S. Marques, et al., Oligodendrocyte heterogeneity in the mouse juvenile and adult central nervous system, Science (80-.) 352 (June 6291) (2016) 1326–1329.
[256] S. Jäkel, et al., Altered human oligodendrocyte heterogeneity in multiple sclerosis, Nature 566 (February 7745) (2019) 543–547.
[257] G.S. Tomassy, V. Fossati, How big is the myelinating orchestra? Cellular diversity within the oligodendrocyte lineage: facts and hypotheses, Front. Cell. Neurosci. 8 (July) (2014) 201.
[258] A. Suzumura, S. Bhat, P.A. Eccleston, R.P. Lisak, D.H. Silberberg, The isolation and long-term culture of oligodendrocytes from newborn mouse brain, Brain Res. 324 (December 2) (1984) 379–383.
[259] T. Jin, S. Yan, J. Zhang, D. Yuan, X.-F. Huang, W. Li, A label-free and high-throughput separation of neuron and glial cells using an inertial microfluidic platform, Biomicrofluidics 10 (May 3) (2016) 034104.
[260] Y. Chen, et al., Isolation and culture of rat and mouse oligodendrocyte precursor cells, Nat. Protoc. 2 (May 5) (2007) 1044–1051.
[261] R.W. O'Meara, S.D. Ryan, H. Colognato, R. Kothary, Derivation of enriched oligodendrocyte cultures and oligodendrocyte/neuron myelinating co-cultures from post-natal murine tissues, J. Vis. Exp. (August 54) (2011).
[262] J.A. García-León, et al., SOX10 single transcription factor-based fast and efficient generation of oligodendrocytes from human pluripotent stem cells, Stem Cell Rep. 10 (February 2) (2018) 655–672.
[263] P. Li, M. Li, X. Tang, S. Wang, Y.A. Zhang, Z. Chen, Accelerated generation of oligodendrocyte progenitor cells from human induced pluripotent stem cells by forced expression of Sox10 and Olig2, Sci. China Life Sci. 59 (November 11) (2016) 1131–1138.
[264] M. Caiazzo, Y. Okawa, A. Ranga, A. Piersigilli, Y. Tabata, M.P. Lutolf, Defined three-dimensional microenvironments boost induction of pluripotency, Nat. Mater. 15 (March 3) (2016) 344–352.
[265] K. Ishihara, E.M. Tanaka, Spontaneous symmetry breaking and pattern formation of organoids, Curr. Opin. Syst. Biol. 11 (October) (2018) 123–128.
[266] L. Ye, C. Swingen, J. Zhang, Induced pluripotent stem cells and their potential for basic and clinical sciences, Curr. Cardiol. Rev. 9 (February 1) (2013) 63–72.
[267] M. Madhavan, et al., Induction of myelinating oligodendrocytes in human cortical spheroids, Nat. Methods 15 (September 9) (2018) 700–706.
[268] G. Nzou, et al., Human cortex spheroid with a functional blood brain barrier for high-throughput neurotoxicity screening and disease modeling, Sci. Rep. 8 (December 1) (2018) 7413.
[269] A.S. Monzel, et al., Derivation of human midbrain-specific organoids from

neuroepithelial stem cells, Stem Cell Rep. 8 (May 5) (2017) 1144–1154.
[270] Y. Zhang, et al., Purification and characterization of progenitor and mature human astrocytes reveals transcriptional and functional differences with mouse, Neuron 89 (January 1) (2016) 37–53.
[271] S.A. Sloan, et al., Human Astrocyte Maturation Captured in 3D Cerebral Cortical Spheroids Derived From Pluripotent Stem Cells, (2017).
[272] W. Zheng, Q. Li, C. Zhao, Y. Da, H.-L. Zhang, Z. Chen, Differentiation of glial cells from hiPSCs: potential applications in neurological diseases and cell replacement therapy, Front. Cell. Neurosci. 12 (August) (2018) 239.
[273] C. McKee, G.R. Chaudhry, Advances and challenges in stem cell culture, Colloids Surf. B Biointerfaces 159 (November) (2017) 62–77.
[274] A. Espinosa-Jeffrey, P.M. Paez, V.T. Cheli, V. Spreuer, I. Wanner, J. de Vellis, Impact of simulated microgravity on oligodendrocyte development: implications for central nervous system repair, PLoS One 8 (12) (2013) e76963.
[275] A. Arani, et al., Acute pressure changes in the brain are correlated with MR elastography stiffness measurements: initial feasibility in an in vivo large animal model, Magn. Reson. Med. 79 (February 2) (2018) 1043–1051.
[276] H. Tzschätzsch, B. Kreft, F. Schrank, J. Bergs, J. Braun, I. Sack, In vivo time-harmonic ultrasound elastography of the human brain detects acute cerebral stiffness changes induced by intracranial pressure variations, Sci. Rep. 8 (1) (2018) 17888.
[277] F. Heath, S.A. Hurley, H. Johansen-Berg, C. Sampaio-Baptista, Advances in non-invasive myelin imaging, Dev. Neurobiol. 78 (February 2) (2018) 136–151.
[278] R.K. Paradise, M.J. Whitfield, D.A. Lauffenburger, K.J. Van Vliet, Directional cell migration in an extracellular pH gradient : a model study with an engineered cell line and primary microvascular endothelial cells, Exp. Cell Res. 319 (4) (2013) 487–497.
[279] M.H. Zaman, et al., Migration of tumor cells in 3D matrices is governed by matrix stiffness along with cell-matrix adhesion and proteolysis, Proc. Natl. Acad. Sci. 103 (29) (2006).
[280] B. Qing, K.J. Van Vliet, Hierarchical design of synthetic gel composites optimized to mimic the impact energy dissipation response of brain tissue, Mol. Syst. Des. Eng. (2016).